5-2012

Synthesis of Gallium Nitride by Laser-Assisted Metal Organic Vapor Phase Epitaxy

Matthew J. Mitchell
University of Nebraska- Lincoln, mattmitchell77@gmail.com

Synthesis of Gallium Nitride by Laser-Assisted Metal Organic Vapor Phase Epitaxy

by

Matthew J. Mitchell

A THESIS

Presented to the Faculty of
The Graduate College at the University of Nebraska
In Partial Fulfillment of Requirements
For the Degree of Master of Science

Major: Electrical Engineering

Under the Supervision of Professor Yongfeng Lu

Lincoln, NE

May, 2012

Synthesis of Gallium Nitride by Laser-Assisted Metal Organic Vapor Phase Epitaxy

Matthew J. Mitchell, M.S.

University of Nebraska, 2012

Advisor: Yongfeng Lu

For the past two decades, gallium nitride (GaN) has become one of the most studied materials in the fields of optics and electronics due to its unique properties. Currently available methods for the synthesis of GaN require a high substrate temperature of 1100 ^{o}C, which can lead to several issues including a high defect concentration and increased probability of cracking and warping of films due to differences in thermal expansion coefficients between the substrate and film. The high growth temperature also prevents the integration of GaN devices with CMOS fabrication techniques, which has a post-process temperature limit of ~575 ^{o}C. Accordingly, there is a need for a low-temperature synthesis technique such as laser-assisted metal organic vapor phase epitaxy (L-MOVPE) to combat these issues. By using a carbon dioxide (CO_2) laser as the energy source for MOVPE, localized heating can be achieved, which lowers the overall substrate temperature.

Over the course of this project, an L-MOVPE system was designed and built, and experiments were carried out to synthesize various morphologies of GaN nanostructures at low substrate temperatures. The results show the L-MOVPE is capable of producing GaN nanowires with lengths up to 2 μm, and widths around 2 nm. Crystal structures were

grown in all sizes ranging from 40 nm to 40 μm, all of which displayed prominent A_1(LO) and E_{2H} peaks, indicating high quality GaN. The largest crystal was found to have a growth rate of ~ 500 to 600 μm/hour, which is significantly higher than growth rates associated with conventional methods. In addition to films and nanowires, other nanostructures including nano-pillars, nano-flowers, and patterned GaN crystals were also grown, all at substrate temperatures ranging from 550 to 850 ^{o} C. These results are significant, because they show that through L- MOVPE, it is possible to achieve low-temperature growth of GaN. The low-temperature method allows GaN synthesis to be efficiently paired with current CMOS techniques, significantly increasing its potential applications in electronics.

Acknowledgements

I would like to thank my adviser, Dr. Yongfeng Lu, for giving me the opportunity to work in his lab, and for his support throughout my Master's program. Thank you to Dr. Premkumar Thirugnanam for the help and guidance given during my experiments and writing of my thesis. I also express my thanks to Dr. Yunshen Zhou, Wei Xiong, Zhiqiang Xie, and everyone working in the LANE Lab for not only being willing to help me work through problems and answer questions, but for making my time in the lab fun and enjoyable. Special thanks to Drs. Dennis Alexander and Mathias Schubert for being on my graduate committee. Finally, I would like to thank my mom, dad, and sister for teaching me the importance of a good education, and always being there to encourage me.

Table of Contents

List of Figures

Chapter 1

Chapter 2

Chapter 3

Chapter 4

List of Tables

Chapter 1

Introduction

Semiconductor materials are the backbone for modern electronics. From light-emitting diodes (LEDs) [1], to the transistors making up computer chips [2], semiconducting materials are at work in just about every aspect of daily life. A specific group of semiconductors, called III-V semiconductors, are particularly sought after for use in optoelectronics because of their wide, direct bandgaps, and high carrier mobilities [3,4]. The label 'III-V' comes from the fact that these materials are made of compounds with one element from Column III of the periodic table, and one element from Column V. Out of the III-V semiconductors, gallium nitride (GaN) has piqued the interest of scientists and engineers due to its unique physical and optical properties.

1.1 Properties of GaN

GaN is a III-V semiconductor made up of the post-transition metal gallium, and non-metal nitrogen. GaN has a wurtzite crystal structure, which can be seen in Fig. 1.1 [5]. GaN has a high heat capacity, a high breakdown field of 5×10^6 V/cm, and a high thermal conductivity of 2.3 W/(cm×K) [2]. This means GaN is physically a very strong material

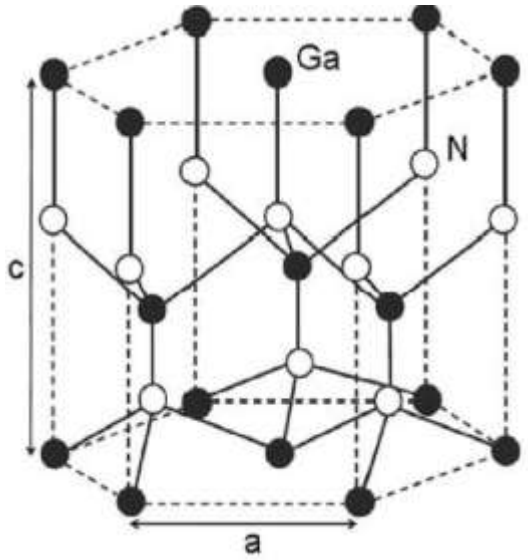

Figure 1.1. Wurtzite crystal structure of GaN.

that can be used in applications involving high temperatures and powers. It also has excellent optoelectronic properties.

GaN boasts a wide direct bandgap of 3.39 eV at 300 K[6]. The band structure of wurtzite GaN can be seen in Fig. 1.2 [3]. A material with a direct bandgap can emit photons because there is no momentum change when an electron moves between the valence and conducting bands. Using Eq. 1.1-1, where *h* is Planck's constant, *c* is the speed of light, and the photon energy is 3.39 eV, one is able to determine the bandgap

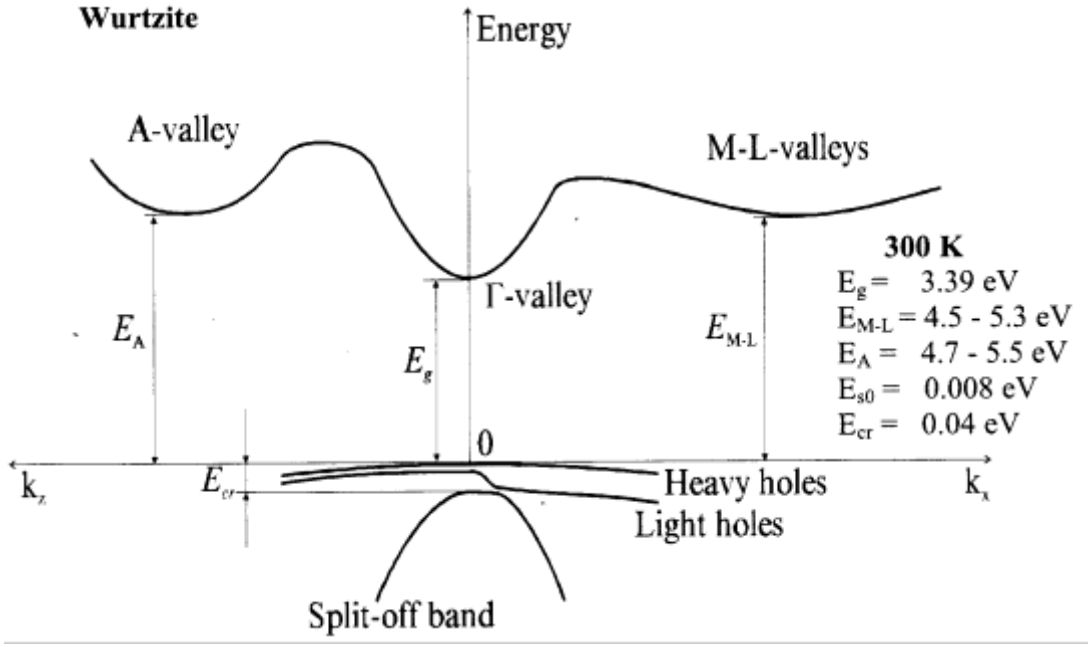

Figure 1.2. Band structure of wurtzite GaN.

wavelength of GaN to be 365 nm. This means the shortest wavelength that pure GaN can emit is 365 nm, which is in the ultraviolet (UV) range of the spectrum [3,4].

$$\textbf{\textit{Photon Energy}} = {}^{hc}/_{\lambda} \qquad \textbf{(1.1-1)}$$

The electron mobility in GaN is <1000 $cm^2/V\times s$. This is not extraordinary when compared with GaAs (<8500 $cm^2/V\times s$) or InN (<3200 $cm^2/V\times s$), but is still relatively high when compared with other materials such as AlN (<300 $cm^2/V\times s$)[3]. High electron mobility allows GaN to be used in high- frequency applications. Table 1.1 shows the properties of some common III-V semiconducting materials [3,4]. It can be seen that GaN is not superior to every material with all of its properties, but overall it proves to have characteristics that give GaN strong potential for many applications.

Table 1.1. Properties of common III-V semiconductors

Material	GaN	GaN	AlN	InN	GaAs
Structure	wurtzite	zinc blende	wurtzite	wurtzite	zinc blende
Bandgap energy (eV)	3.39	3.2	6.2	~0.7	1.42
Bandgap type	direct	direct	direct	direct	direct
Effective electron mass (m_0)	0.2	0.13	0.4	0.055	-
Electron affinity (eV)	4.1	4.2	0.6	-	-
Lattice constants (A)	a=3.189 c=5.186	4.52	a=3.112 c=4.982	a=3.533 c=5.693	565.35
Breakdown field (V/cm)	5×10^6	5×10^6	1.2×10^6	-	4×10^5
Electron mobility (cm^2/(V×s))	<1000	<1000	300	<3200	<8500
Hole mobility (cm^2/(V×s))	<200	<350	14	<80	<400
Thermal conductivity (W/(cm×C))	1.3	1.3	2.85	0.45	0.55

1.2 Applications

Due to these unique physical and electrical properties, GaN has found itself being used in a wide range of applications. As the global community works to phase out inefficient incandescent light bulbs, there has been a surge in usage of solid-state lighting sources such as light emitting diodes (LEDs). An issue that has plagued LED lighting is the inability to efficiently achieve long-lasting blue LEDs which, when combined with readily available red and green light sources, creates white light[8]. As previously calculated, pure GaN is capable of achieving light in the UV region, but proper doping with Al, Mg, and In allows GaN- based materials to achieve a range wavelengths from UV to IR[1]. This wide range of wavelengths makes GaN a prime candidate not only for

solid-state light bulbs, but also for applications in televisions, computer monitors, and displays[8].

In addition to LEDs, GaN can also be used to make violet laser diodes. Violet laser diodes with a wavelength of 473 nm were traditionally made by using a beta Barium borate (BBO) crystal to frequency double the 946 nm output of an Nd:YAG crystal[9]. GaN-based violet lasers range in wavelength from 405 to 450 nm, and generate this wavelength without frequency doubling, making them more efficient[10]. Because of their short wavelength, GaN-based violet laser diodes are often used in data storage applications; most famously for reading densely packed Blu-Ray discs[11]. Several GaN applications can be seen in Fig. 1.3 [12-15].

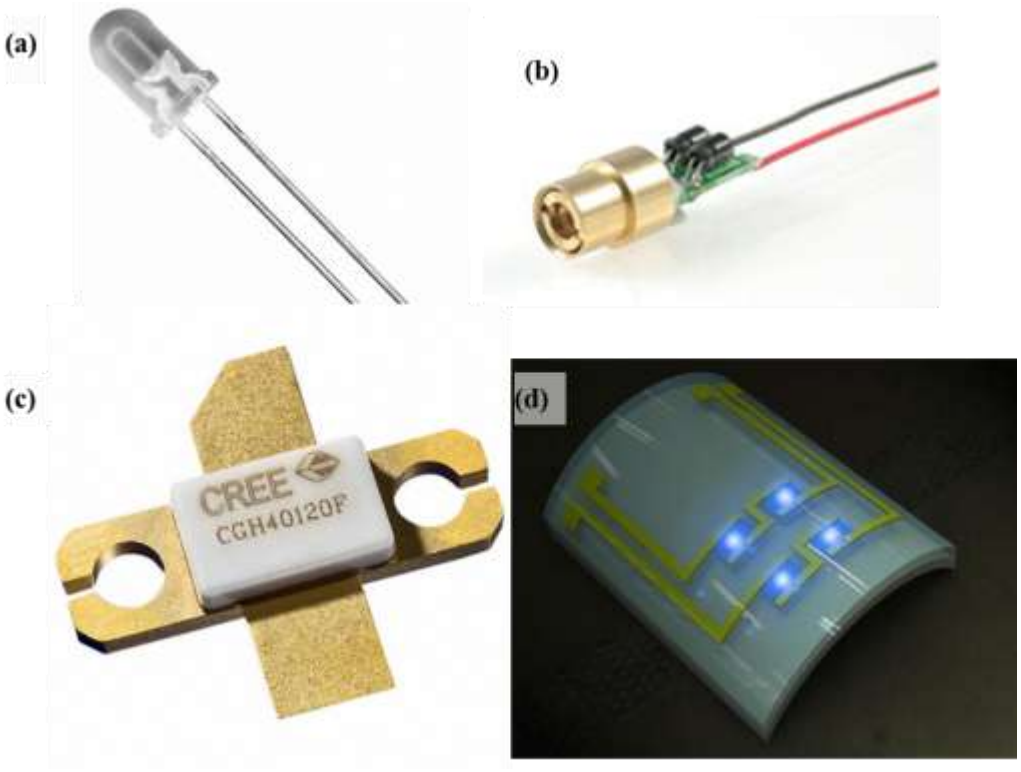

Figure 1.3. Applications of GaN in (a) LED, (b) GaN blue laser diode (c) HEMT, (d) heart monitor bio-sensor.

GaN has also made its way into the world of transistors. Its high electron mobility (two-dimensional electron gas) lends it to application in high electron mobility transistors (HEMTs), which are used primarily in high-frequency telecommunication[17]. Its high thermal conductivity, heat capacity, and breakdown voltage makes GaN an excellent candidate for high temperature and power applications such as high-voltage switches for power grids, and microwave emitters for microwave ovens[17]. GaN-based metal-oxide-semiconductor field-effect transistors (MOSFET) have already found use in high power control systems for hybrid and electric vehicles[2].

Finally, GaN is biocompatible. It has the potential to be used for electronics and sensors that are embedded into living organisms[16]. Overall, GaN is one of the most versatile, promising materials currently being studied. From lasers to microwaves, electric cars to bio-sensors- GaN has potential to improve optoelectronics in just about every field [18].

1.3 Synthesis

There are many methods available for synthesizing GaN including, but not limited to, liquid phase epitaxy (LPE), molecular beam epitaxy (MBE), hydride vapor phase epitaxy (HVPE), and metal organic vapor phase epitaxy (MOVPE). Each method has its pros and cons depending on the quality, and structure of GaN one is trying to achieve, and the application in which it will be used.

MBE is a form of solid phase epitaxy, and is specifically used to achieve epitaxial layers. It is a physical deposition where a source material is heated until it produces an evaporated beam of particles, which condense on a substrate's surface. MBE is conducted

in an ultra-high vacuum (<10^{-10} torr), and deposits very pure, single-crystal layers. MBE is generally a very slow process, with deposition rates around 1 µm/hour[19].

Like MBE, the methods of MOVPE, LPE, and HVPE can used to achieve epitaxial layers. Unlike MBE, these three are chemical reactions between precursors rather than a physical deposition. HVPE involves the reaction of heated metal chlorides with ammonia. It does not require a vacuum, and uses relatively inexpensive precursors. HVPE has reported growth rates as high as 800 µm/hour, but more commonly in the range of 50 µm/hour – 60 µm/hour[20]. LPE is carried out when a substrate is brought into contact with a super-saturated melt of the desired semiconductor material. The melt is then cooled, and layers are formed. An average reported growth rate for LBE is 1 µm/hour, but can vary depending on the materials used [21].

In MOVPE, at least one of the precursors is a metalorganic compound, which is a compound made up of a metal and an organic functional group. Traditional MOVPE systems use a susceptor in order to completely heat the chamber and the substrate inside. This process only requires a vacuum of <10 torr, which is significantly lower than MBE, and for this reason is more commonly used in optoelectronic applications [22]. Table 1.3 shows the strengths and weaknesses of various methods of GaN synthesis [23].

Table 1.2. Synthesis methods

Method	Strengths	Weaknesses
MOVPE	High quality films	Expensive/ hazardous precursors
	Scalable	Many parameters to control
	High deposition rate	
MBE	High quality films	Slow deposition rate
	Simple process	Requires very high vacuum
LPE	High deposition rate	Non-uniform films
	Simple process	Not scalable
HVPE	Large scale	Hazardous precursors
	Inexpensive precursors	Complex process

In the chemical synthesis of GaN via MOVPE, two precursors are used – ammonia (NH_3) is the nitrogen source, and trimethylgallium (TMGa) is the source for gallium. NH_3 is a gas, which can easily be pumped into the chamber. TMGa is a liquid, so in order to get this precursor into the chamber, an inert gas like N_2 is pumped through the TMGa, this gas will carry metalorganic vapor to the reaction site [24]. Heat is used to decompose the precursor molecules into their atomic counterparts, which bond and crystallize on the surface of the substrate [25]. The chemical reaction for the synthesis of GaN is shown in Eq. 1.3-1.

$$Ga(CH_3)_3 + NH_3 \xrightarrow{1000\ ^\circ C} GaN + 3CH_4 \qquad \textbf{(1.3-1)}$$

1.4 Motivation and Goals

The ultimate end result of this project is twofold: to achieve aligned GaN nanowires, doped in a manner to facilitate UV light emission; and to achieve high quality GaN epitaxial layers grown at low substrate temperature. However, due to time limitations of a Master's degree, the project had to be broken down into a more manageable size. The specific objective of this thesis is to design and build an L-MOVPE system capable of growing GaN nanostructures and thin films at low temperatures. Then, by studying how various parameters such as precursor flow rates, catalysts, and chamber pressure affect the morphology, quality, and growth rate of the GaN, come up with optimized growth parameters for the various structures. This research will lay the groundwork for the overall project goals mentioned above.

As stated previously, in conventional MOVPE, a relatively high substrate temperature (~1100 ºC) [26] is needed in order to facilitate growth of GaN. This is because traditional MOVPE relies on convection for the thermal decomposition of NH_3, the nitrogen source. Three problems arise as a result of this high growth temperature: 1) a large number of defects in the epitaxial layer due to lattice mismatch between the film and the substrate[27], 2) warping and cracking of the films due to differences in the thermal expansion coefficients of the materials[28], and 3) MOVPE cannot be incorporated into current CMOS techniques, which can only withstand post-processing temperatures up to ~575 ºC [29]. In addition to the problems associated with high temperatures, MOVPE techniques have only been shown to be capable of reaching growth rates of ~20 µm/hour[26]. While this is better than some methods like MBE, it is still relatively slow when compared with methods like HVPE. In order for GaN to be

widely employed in commercial applications, developments need to be made to these key areas.

A laser-based MOVPE technique was chosen to improve upon the shortcomings of traditional MOVPE. The CO_2 laser will enable GaN growth at lower substrate temperature because of localized heating of the sample. With localized heating, the maximum temperature is only reached inside the laser spot, meaning the rest of the substrate remains at a lower temperature. By lowering the synthesis temperature, L-MOVPE takes a step toward a synthesis method that is compatible with the post-processing temperature limitations of current CMOS fabrication techniques, and will allow for integration of GaN and CMOS devices without needing to change the current semiconductor fabrication infrastructure.

When using convection heating, the whole chamber is heated, and time is spent waiting for the substrate to reach the desired experimental temperature, which can take several minutes. At the conclusion of the experiment, cooling can take upwards of an hour[22]. The laser-based method uses a laser focused directly on the sample, meaning only the substrate is heated - time and energy is not wasted heating up the entire chamber. Using this method, experimental temperature is reached in a matter of seconds[30]. When the experiment is done, the sample can completely cooled in about five minutes. This rapid heating and cooling greatly reduce the synthesis time.

Chapter 2

Experimental Implementation

As described in the previous chapter, laser-assisted metal organic vapor phase epitaxy (L-MOVPE) offers a potential solution to the shortcomings of conventional synthesis methods such as MOVPE, MBE, and HVPE. In this chapter, the execution of the project will be laid out. Firstly, the design and construction of the L-MOVPE will be reported, followed by the steps taken to prepare several different types of samples used in the experiment. Finally, the experimental process will be discussed in a step-by-step fashion.

2.1 Experimental Setup

A laser-assisted metal organic vapor phase epitaxy (L-MOVPE) system was built in-house. Inside a vacuum chamber, a substrate (e.g. Si/SiO2) was held to a ceramic stage via a tungsten wire sample holder. Figure 2.1 shows the sample holder. The ceramic holder is used to thermally isolate the sample from the metal chamber. Also, a BNC connector can be seen at the top of the sample holder. This can be used to incorporate a thermo coupler for temperature monitoring, or to apply a DC bias to the sample via the tungsten sample holder. A 40 watt Synrad Firestar V40 CO_2 laser with wavelength of 10.6 μm was aligned through a window to focus on the center of the sample. The NH_3 gas flow was directly controlled using an Alicat MCS-2000 mass flow controller (MFC), which can be set as high as 2000 sccm. Manipulation of the metal organic precursor,

Figure 2.1. Ceramic sample stage.

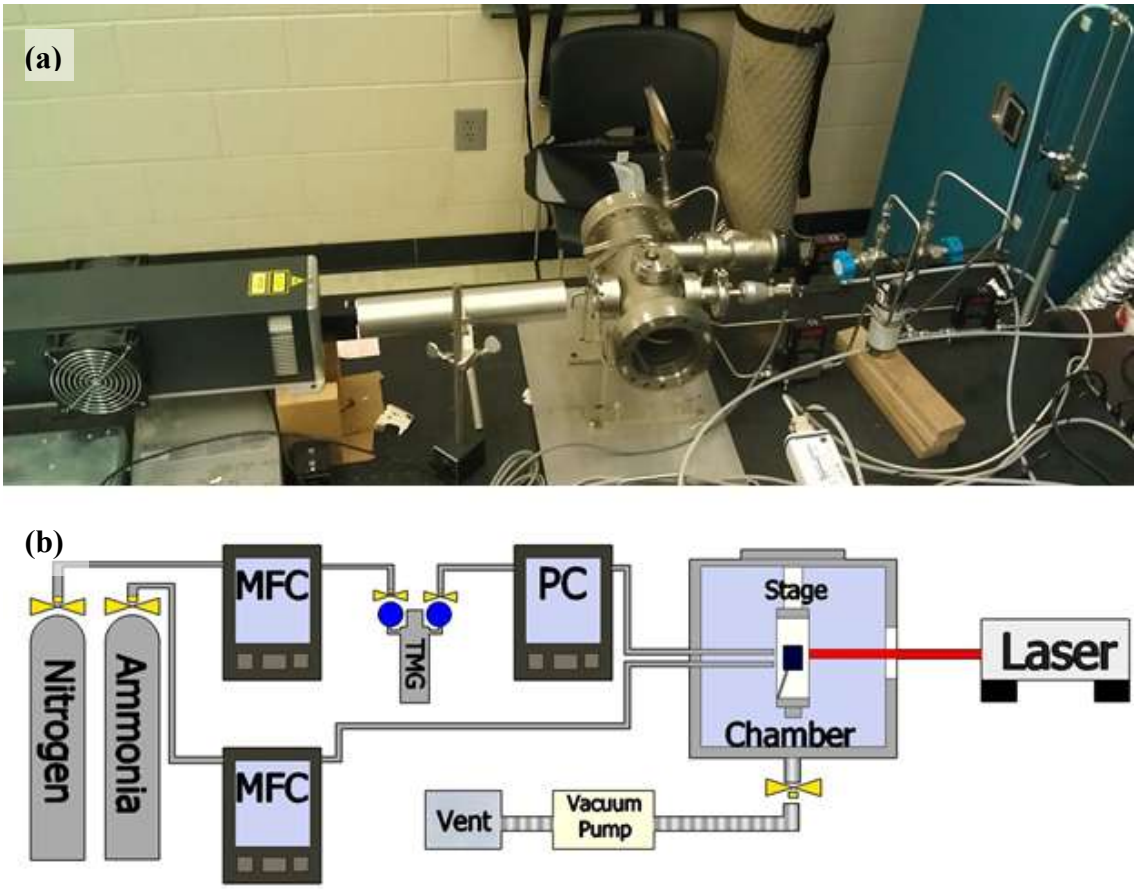

Figure 2.2. Experimental setup showing (a) actual implementation of system and (b) schematic diagram of the system.

TMGa, is slightly more complicated. Nitrogen, which is used as the carrier gas for gallium, uses an Alicat MCS-20 MFC (range: 20 sccm) to control its flow rate, is sent through a bubbler (AkzoNobel) containing TMGa. On the downstream of the bubbler an Alicat PCS-30 pressure controller (PC) is used to control the amount of TMGa going into the chamber. The NH_3 and TMGa were sent into the chamber through separate ¼" stainless steel pipes. Independent pipes were used in order to prevent gases from mixing in the pipe and forming a solid, which could eventually clog the path. The chamber pressure is monitored using a senTorr Varian BA2C pressure gauge, and adjusted using a valve connected to an Alcatel vacuum pump. The temperature was measured using a

pyrometer (Omega Omegascope OS3750), which was aimed at the sample through a view-port. Fig. 2.2 (a) shows the real-life implementation of the experimental setup and Fig. 2.2 (b) shows the schematic representation of the L-MOVPE system.

2.2 Sample Preparation

Four types of substrates were used in the experiments: bare Si, Si with a SiO_2 layer, Si/SiO_2 sputtered with a catalyst metal, and patterned Si substrates. The Si/SiO_2 wafers are p-type, (100) oriented, and 500 µm-550 µm thick, with a 2 µm-thick layer of SiO_2. The Si wafer is also (100) oriented and 275 µm thick. The first step of preparation was cutting the 4" wafers down into 1 cm × 1 cm square substrates. The SiO_2 substrates were sonicated in an acetone bath for five minutes to remove any contamination from the sample. For Si substrates, an addition bath administered in 10% HF solution for 2 minutes. This was done immediately preceding the experiment in order to remove any thin coating of SiO_2 that may have formed on their surface.

In order to create a pattern on some samples, photolithography was used. Samples were coated with S1813 photoresist using a Laurell WS-650SZ spin coater. The samples were spun at 4000 rpm for 30 seconds, then baked at ~100 ºC for 150 sec. Next, the samples were aligned under a lithography mask using an Oriel 83210 mask aligner. The samples were exposed to 200 W of UV light for 10-15 sec using an Oriel 97435 UV lamp. When the exposure was complete, the samples were developed for 30- 50 seconds using CD-30 developer. Samples were checked under a microscope to ensure the patterns were of good quality and ready for sputtering. Patterns were designed using Cadence layout software, and contained a pair of four large pads, used to make electrical

contact. Each set of pads was connected to a set of sharp tips. The sharp tips had a spacing that varied from 5 to 20 µm. This pattern was designed in order to allow for the growth and measurement of GaN nanowire bridges, and can be seen in Fig. 2.3 (b). Figure 2.3 (a) shows an image of the pattern obtained by an optical microscope.

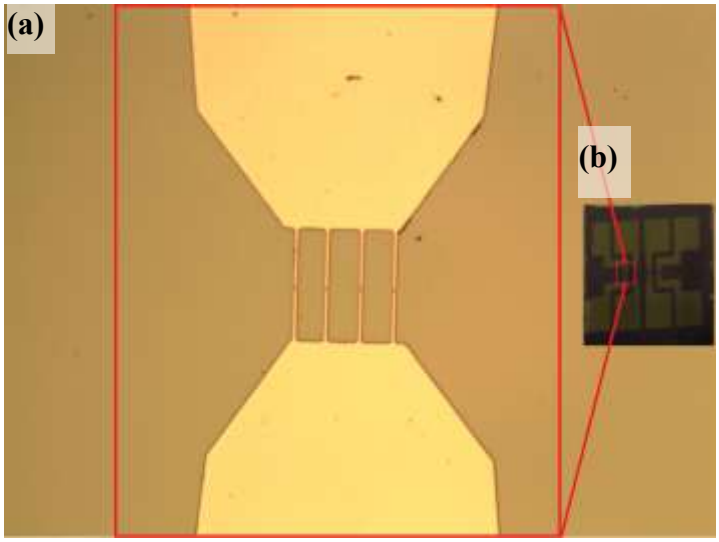

Figure 2.3. Patterned Si substrate. Image shows (a) an optical microscope image of completed pattern and (b) a macroscopic view of a sample.

For the samples (both patterned and non-patterned) that needed metal coatings, an ATC 2000-F sputtering system (AJA International) was used to apply metal thin-films to the substrates. The non-patterned substrates were uniformly coated with an Au thin film ranging from 0.8 nm to 10 nm in thickness. For the patterned substrates, an Al/Fe/Al or Al/Au/Al bimetallic catalyst was applied to the top of a 200-nm-thick molybdenum base layer. The Al and Au layers were sputtered using a 300-W AJA-A600RF RF power supply set to 60 W. The Fe and Mo layers were applied using a 750-W AJA-DCXS DC power supply set to 75 W. The Mo base was to be used as an electrode to provide a way to measure electrical properties of the synthesized materials, the Fe or Au served as

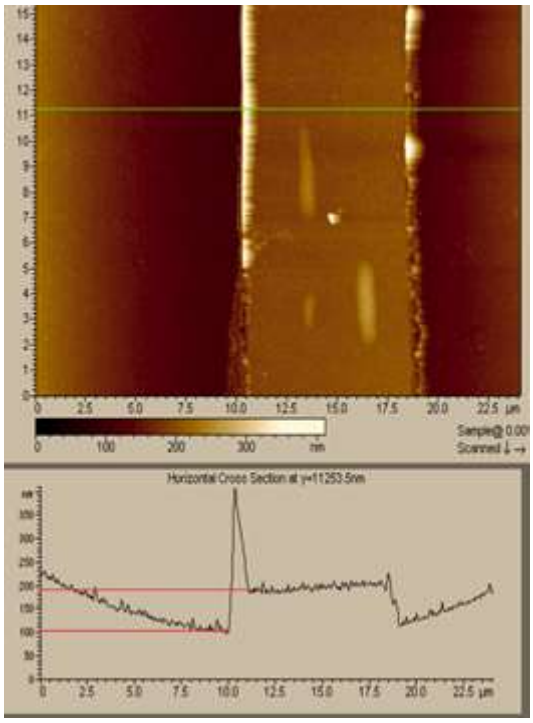

Figure 2.4. Atomic force microscope image of a patterned metal electrode.

active catalysts, and the Al served as a buffer layer and encouraged the formation of isolated catalyst nanoparticles. The film thicknesses were measured using an atomic force microscope (Agilent Technologies AFM5500) in order to determine the sputtering deposition rate of each metal, and calibrate the system. Figure 2.4 shows an AFM micrograph of a deposited metal layer.

2.3 Experimental Execution

To begin each experiment, one of the prepared samples was secured to the ceramic sample stage using a tungsten sample holder. The stage was placed in the vacuum chamber, and the chamber was brought down to 1 mTorr pressure. Because TMGa is pyrophoric, it was necessary to make sure no oxygen was present in the

chamber. To ensure this, the chamber was flushed with nitrogen three times by bringing the chamber up to 760 Torr with nitrogen, and then pumping it down to 1 mTorr.

Once the chamber was flushed and brought down to a final pressure of 1 mTorr, the precursor gasses were let into the chamber. First, the MFC which controls the NH_3 was programmed to and given time to reach the desired set point. Next, the MFC which controls the N_2 flow through the TMGa bubbler and the PC which controls the pressure of the TMGa entering the chamber were programmed to their respective set points. Finally, the TMGa bubbler was opened to allow the nitrogen to flow through and time was allotted to let both the MFC and PC reach their set points.

When both precursor gases were flowing at the set rate, the chamber pressure could be controlled by slightly opening or closing the vacuum valve. After the desired

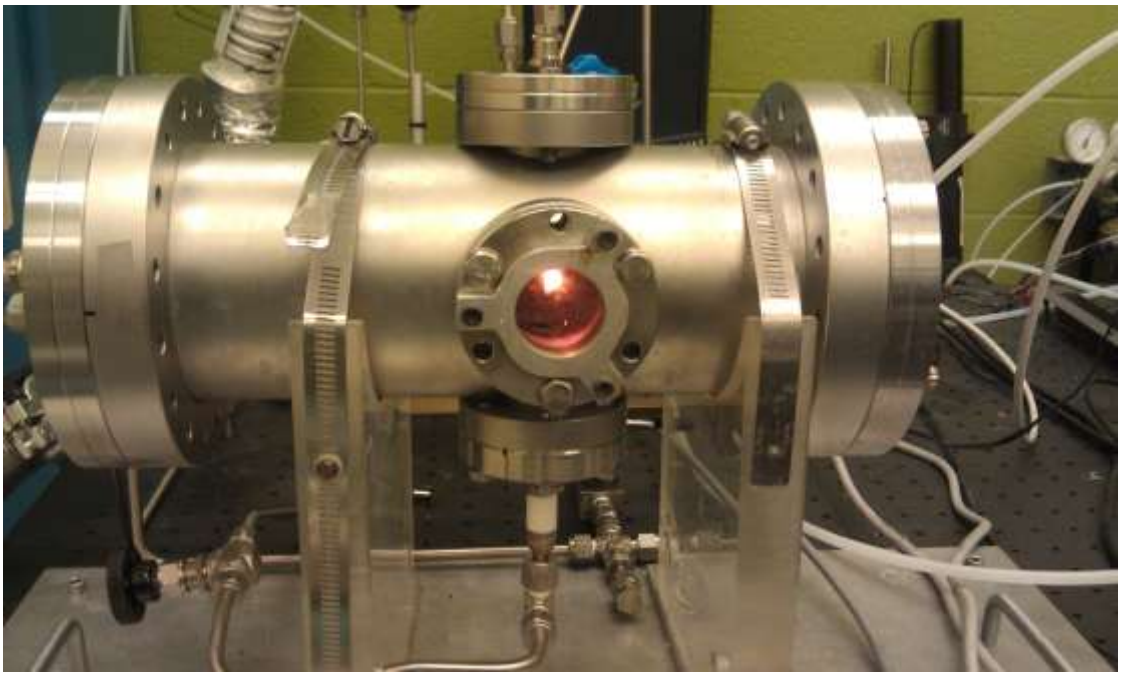

Figure 2.5. Image of chamber during experiment. Si substrate heated to 850 ºC can be seen glowing inside.

chamber pressure was reached, the CO_2 laser was turned on in order to heat the sample. Due to the small size of the samples, the experimental temperature was reached in a matter of seconds. The experiment timer was started as soon as the desired temperature was reached. During the experiment, chamber pressure, flow rates of the precursor gasses, and substrate temperature were all monitored and adjusted as need to maintain the desired experimental parameter. Figure 2.5 shows the chamber during an experiment. The 850 ºC Si substrate can be seen glowing inside.

At the conclusion of the experiment, the laser power was turned off, the TMGa bubbler was closed, the valves of the MFCs and PC were closed, and the vacuum valve was completely open. The chamber was allowed to pump down to 1 mTorr and left to sit for 3-5 min. This time allowed the remaining precursor gases to be pumped out, and gives the sample time to cool. After cooling, the chamber was once again flushed with nitrogen three times in order to make sure all TMGa was evacuated from the chamber before opening it. Finally, the chamber was vented with nitrogen, the sample was removed from the stage, and taken for further characterization.

2.4 Characterization Techniques

After the experiment, the samples were subject to several different characterization methods. Field-emission scanning electron microscopy (FE-SEM) and transmission electron microscope (TEM) were used to view the morphology and orientation of the synthesized structures. Raman spectroscopy, laser-induced breakdown spectroscopy (LIBS), and energy-dispersive x-ray spectroscopy (EDX) were used to examine the crystallinity and composition of the samples.

2.4.1 Micro-Raman Spectroscopy

Raman spectroscopy is a method that uses inelastic Raman scattering to detect low frequency modes in materials. For the most part, when photons are scattered from molecules, the scattered and incident photons have the same wavelength and energy. This elastic scattering is called Rayleigh scattering. In a small number of instances (10^{-5} %)[31], the photon is scattered with excitation, and therefor has a different energy and wavelength than the incident photon. This occurs when the incident photon interacts with the bonds of a molecule. The energy from the photon causes the molecule, which is in a ground state, to excite into a virtual energy state. When the molecule returns to the ground state, a photon with different energy is emitted. This is called Raman scattering, and is the basic principle behind Raman spectroscopy. In a Raman spectroscope, the sample is illuminated with a laser beam. The light reflected from the sample is collected

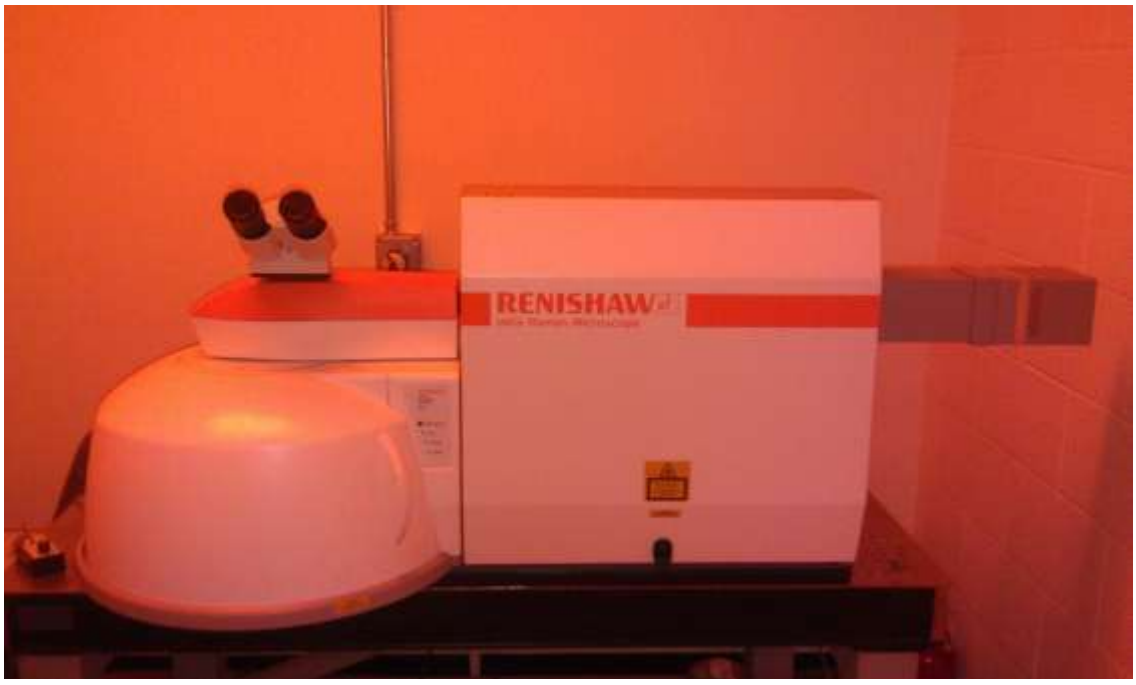

Figure 2.6. Renishaw inVia micro-Raman Spectroscope.

through a lens, and then put through a notch filter in order to filter out the photons near the wavelength of the incident beam, which were elastically scattered. The remaining photons have either been shifted to a lower frequency, which is called a Stokes shift, or to a higher frequency, which is known as an Anti-Stokes shift[31]. The Raman system used was a Renishaw inVia Raman microscope. The samples were loaded, and viewed at either 20× or 50× magnification under atmospheric pressure. The laser used for the Raman characterization was an Ar-ion laser (Modu-Laser StellerRen 50 mW) with a wavelength of 514 nm. The micro-Raman system can be seen in Fig. 2.6.

2.4.2 Field-Emission Scanning Electron Microscopy (FE-SEM)

FE-SEM is a microscopy method that scans a sample with a beam of accelerated electrons in order to image its surface. Traditional SEM systems use thermionically emitted electrons, which come from a heated tungsten filament. An FE-SEM differs in that its source of electrons is a field emission source. A field emission source has a sharply- pointed tip held at a very high (kV) potential to an electrode. The potential is so large that the electrons are released from the tip of the emitter. Once the electrons are released, they are sent through electromagnetic lenses, which are lenses that use varying magnetic fields to deflect and focus the charged particles. After focusing, the beam goes through a series of deflector plates, which are used to scan the beam over the surface of the sample. The electron beam interacts with the sample, and produces secondary electrons, which are picked up, and interpreted by a detector[32]. The FE-SEM used in these experiments was a Hitachi 4700, capable of reaching 500,000× magnification and 1.2 nm resolution. The samples were bombarded with electrons accelerated at 15 kV under a vacuum of 10^{-9} torr. Figure 2.7 shows the FE-SEM system.

Figure 2.7. Hitachi FE4700 Field Emission Scanning Electron Microscope.

2.4.3 Laser-induced Breakdown Spectroscopy (LIBS)

LIBS is an atomic emission spectroscopy used to determine the composition of materials. The basic principle behind LIBS is the emission of characteristic wavelengths of light by excited atoms. In LIBS, a high-powered laser is focused on a very small portion of a sample. The high energy from the laser pulse ablates and atomizes the portion of the sample, and creates ultra-high temperature plasma. From this plasma, the characteristic emission lines from the excited atoms can be detected[33]. For LIBS characterization, an excimer laser (Coherent CompEx pro 205F), with a wavelength of 248 nm, power of 240 mJ/pulse, and pulse width of 23 ns was used to breakdown the sample. A spectrometer (Andor Shamrock) was used to collect the data, and Andor Solis software was used to interpret the data. A real-life implementation and schematic view of the LIBS system can be seen in Fig. 2.8.

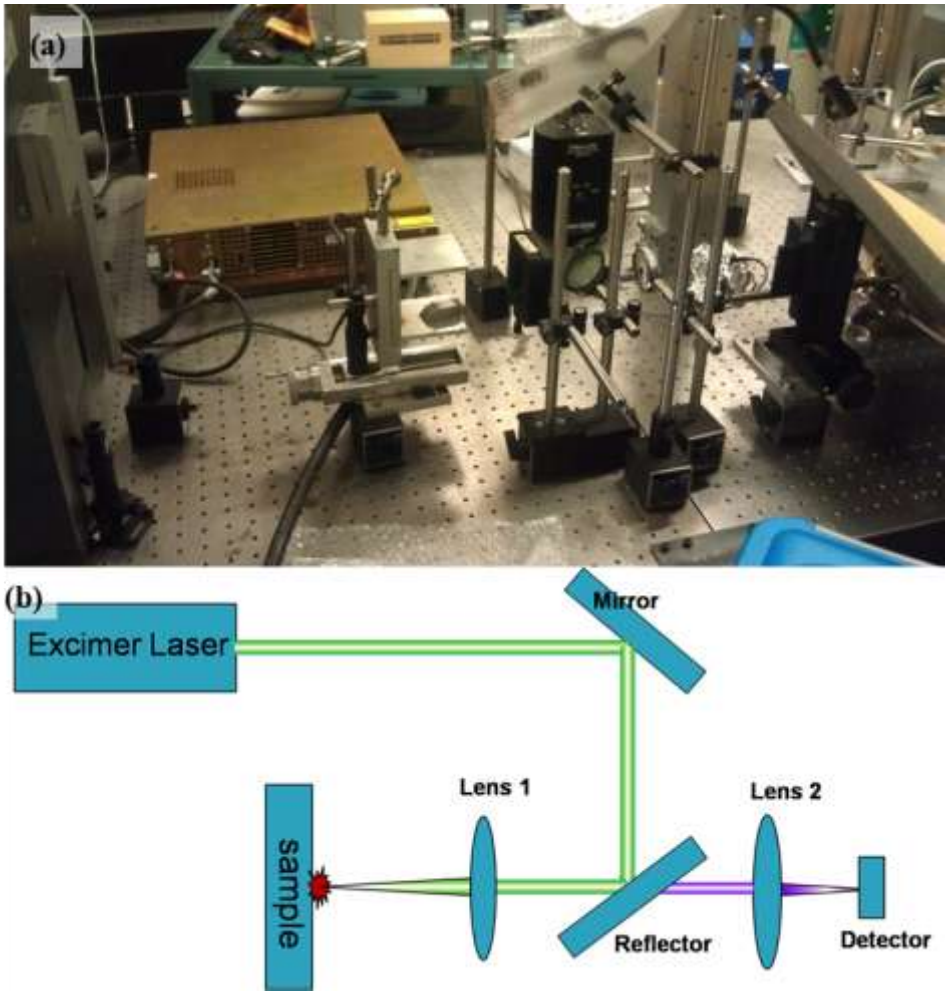

Figure 2.8. (a) Real-life implementation and (b) schematic diagram of LIBS system.

2.4.4 Transmission Electron Microscopy (TEM)

TEM is similar to SEM in that its electron source is also based upon field emission, and the beam is focused using electromagnetic lenses. It differs from SEM because in TEM, the electron beam is transmitted through the sample, rather than just reflected off of it. In TEM, the sample must be relatively thin (200- 500 nm) in order for the electrons to pass thorough. Samples are prepared on a copper mesh and placed under a high vacuum (~10^{-8} Torr) in order to reduce the interaction between electrons and gas

particles to a negligible level. Then the sample is bombarded with an electron beam, which is transmitted through the sample, and picked up by a detector on the other side. There are many ways to develop images from the detected electrons, the most common of which is bright-field imaging. Thicker, more dense areas of the sample absorb more electrons and appear darker in contrast to thinner, less dense areas. Other imaging methods include measuring the electron energy loss, and the phase of the transmitted electrons[31]. In this study, a Tecnai G2 F30 TEM was used. This system has a point resolution of .24 nm, magnification up to 800,000×, and acceleration voltages of up to 300 kV. This resolution, which is higher than the SEM, allows for imaging of the lattice structure of the samples.

Figure 2.9. Tecnai G2 F30 TEM equipped with EDAX PV9900 spectrometer.

The TEM system used was also capable of EDX measurements because of the addition of an EDAX PV9900 spectrometer. In EDX, a high-energy beam of electrons is focused on a sample. The energy from the beam excites the atom, and causes it to eject an

electron from its innermost shell. The vacancy in the inner shell is filled with an electron from a higher-energy outer shell. The difference in energy is released as an X-ray, which is picked up by an X-ray detector. Every element has its own unique peaks in the X-ray spectrum, so based on the characteristic peaks, elemental composition of samples can be determined[34]. The TEM/ EDX setup can be seen in Fig. 2.9.

Chapter 3

Results

Using the experimental setup and techniques described in the previous chapter, different GaN morphologies were achieved. This includes nanowires, nano-flowers, nano-pillars, grain-like crystal structures, and large GaN crystals. In order to properly characterize these samples, techniques like FE-SEM and TEM were used to study the morhpology of the GaN, and methods like EDX, LIBS, and Raman spectroscopy were used to determine the composition and crystallinity of the GaN. The results in this chapter show that the L-MOVPE method is capable of achieving numerous morphologies of high quality GaN at relatively low substrate temperatures.

3.1 GaN Nanostructures

As stated previously, one of the primary goals of this research was the synthesis and study of GaN nanowires, which can be used in many applications. In the attempts to achieve nanowires, varying the growth parameters in the L-MOVPE system lead to the synthesis of many other morphologies of GaN, including nano-pillars, nano-flowers, and grain-like GaN crystals.

3.1.1 GaN Nanowires

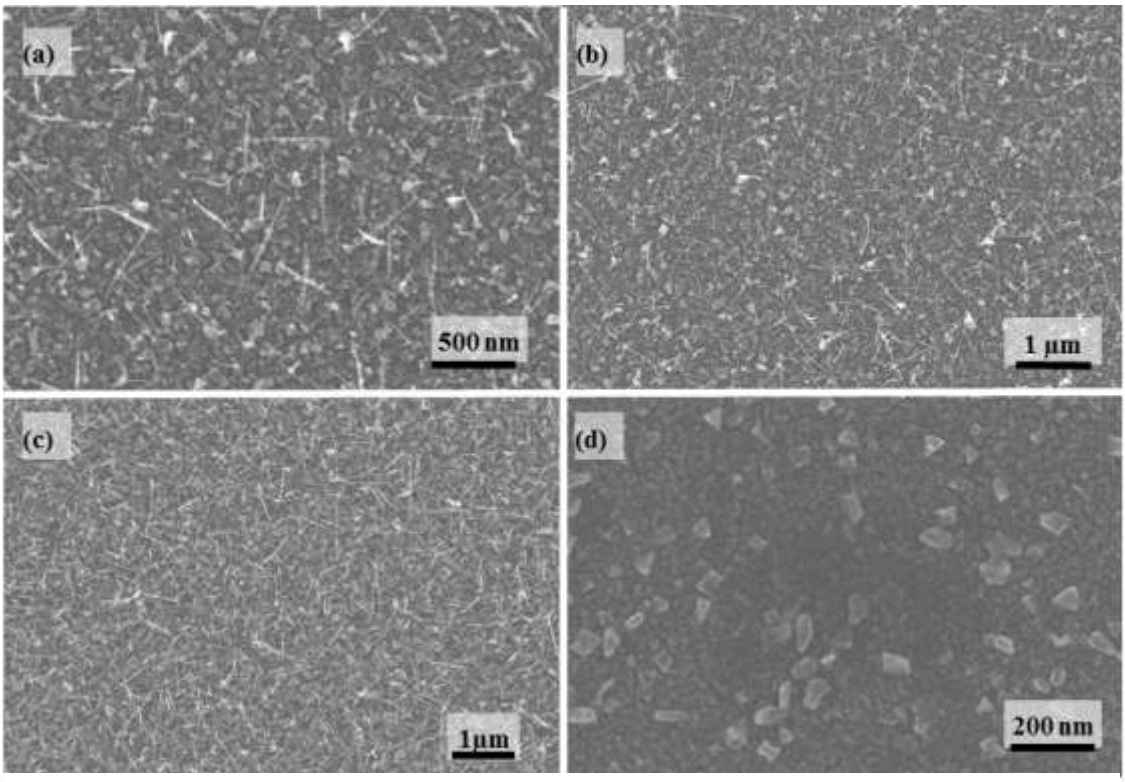

Figure 3.1. SEM image of GaN deposited at (a) 550 (b) 650 (c) 750 and (d) 850 °C on a gold-coated Si/SiO_2 substrate.

GaN nanowires grow through the vapor-liquid-solid (VLS) mechanism[35], so gold-catalyst-coated Si/SiO_2 samples were used in the experiments. The experiments were carried out with the following parameters: NH_3 flow rate of 30 sccm, chamber pressure of 600 Torr, TMGa flow rate of 10 sccm, experimental time of 10 min, and substrate temperature was varied from 550 to 950 ºC. The FE-SEM images for 550 to 850 ºC can be found in Fig. 3.1. Figure 3.2 shows the FE-SEM for 950 ºC. From the micrographs, it can be seen that nanowires are achieved at temperatures as low as 550 ºC, though at this temperature, the nanowires are sparse, and only have a length of around 200 to 500 nm. As the temperature increases to 650 ºC, nanowires are still fairly scant, but have significantly increased in length to around 1– 2 µm. At a substrate temperature of 750 ºC, nanowires are abundant, but the length remains roughly the same as the wires synthesized at 650 ºC. When the temperature was raised to 850 ºC, nanowires are no longer found inside the laser spot. Instead, small crystal structures with diameters ranging from ~10 to 50 nm are seen. Finally, when the temperature reached 950 ºC, the Si/SiO_2 substrate was obliterated, and no nanostructures of any kind were found.

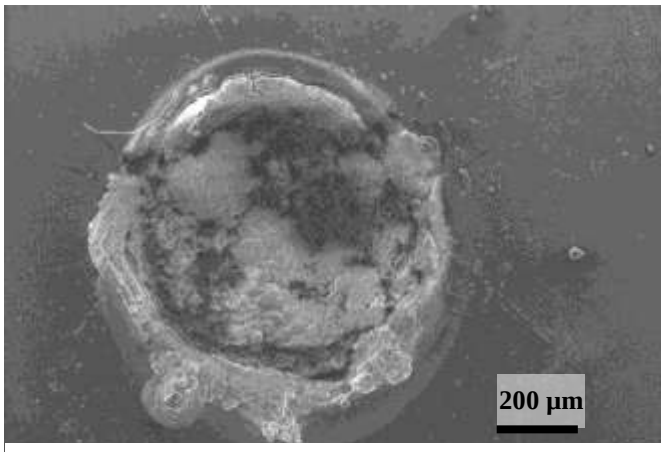

Figure 3.2. Sample obliterated at 950 ºC.

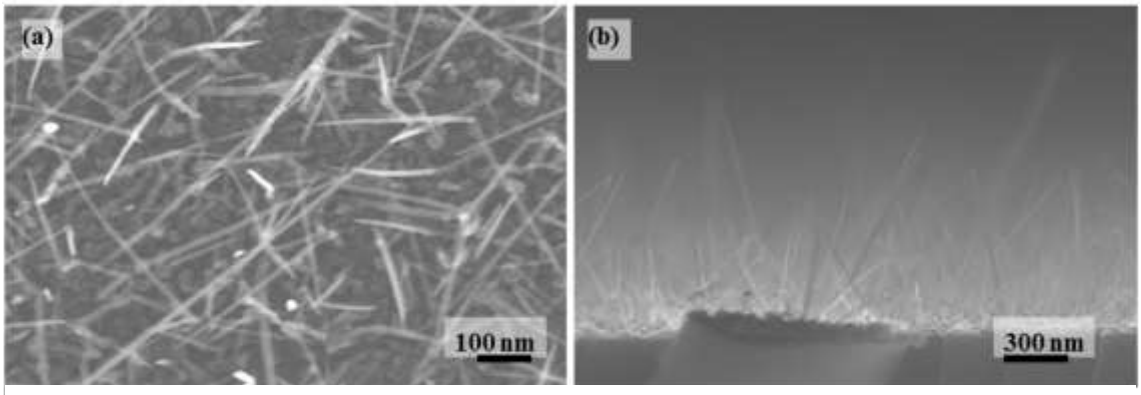

Figure 3.3. (a) Magnified and (b) cross-sectional views of GaN nanowires grown at 750 ºC.

This result showed that the optimum temperature for nanowire growth inside the laser spot is 750 ºC, so for further experiments on the growth of nanowires, this temperature was maintained. Figure 3.3 shows magnified and cross sectional images of nanowires grown at 750 ºC. In Fig. 3.3 (a), the diameter of the nanowires can be seen, and ranges from about 10 to 20 nm. The cross sectional SEM image shows that a majority of the nanowires are vertically aligned, and range in height from 100 nm to about 1.5 μm.

Figure 3.4 shows Raman spectra collected on this sample. The Raman spectrum shows a large A_1(LO) peak at 726 cm^{-1} and a relatively small E_{2H} peak at 570 cm^{-1}. The E_{2H} peak confirms that the nanowires grown are, in fact, GaN, the weakness of the peak suggests that the crystalline quality of the GaN nanowires is low. The large peak at 520 cm^{-1} is a Si peak due to the Si/SiO_2 substrate.

In order to further understand the growth of GaN nanowires, the samples were characterized using high resolution TEM. Micrographs of individual nanowires were obtained and can be seen in Fig. 3.5 (a). The image shows nanowires with a constant

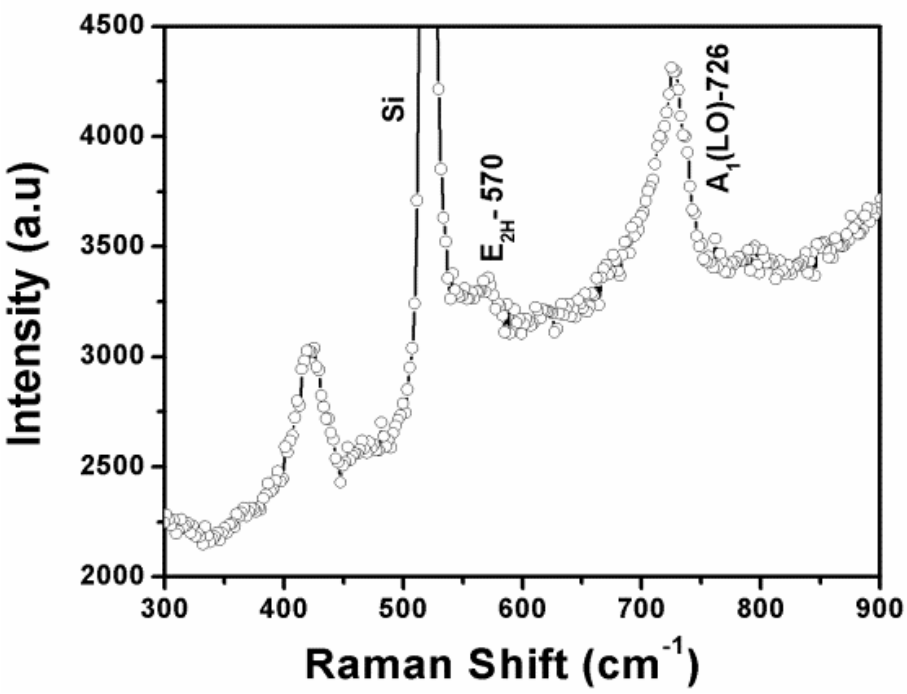

Figure 3.4. Raman spectrum collected from nanowires grown at 750 ºC.

thickness of 50 nm and lengths greater than 250 nm. The lattice structure of the nanowire was also imaged using the TEM. Figure 3.5 (b) shows ~2 Å spacing between the lattice planes, which indicates growth along the c-axis. Finally, EDX was carried out on the nanowire to determine its composition. The EDX result can be seen in Fig. 3.6. The result shows two small gallium peaks and a very large nitrogen peak. This confirms that the nanowires are composed of GaN. Also present are Cu, Si, Al, O, and C. The Si and O peaks are due to the fact that the nanowires were grown on Si/SiO_2 substrates. The Cu peak comes from the fact that the samples were placed on a Cu mesh for TEM measurement. The Al peak is likely due to contamination.

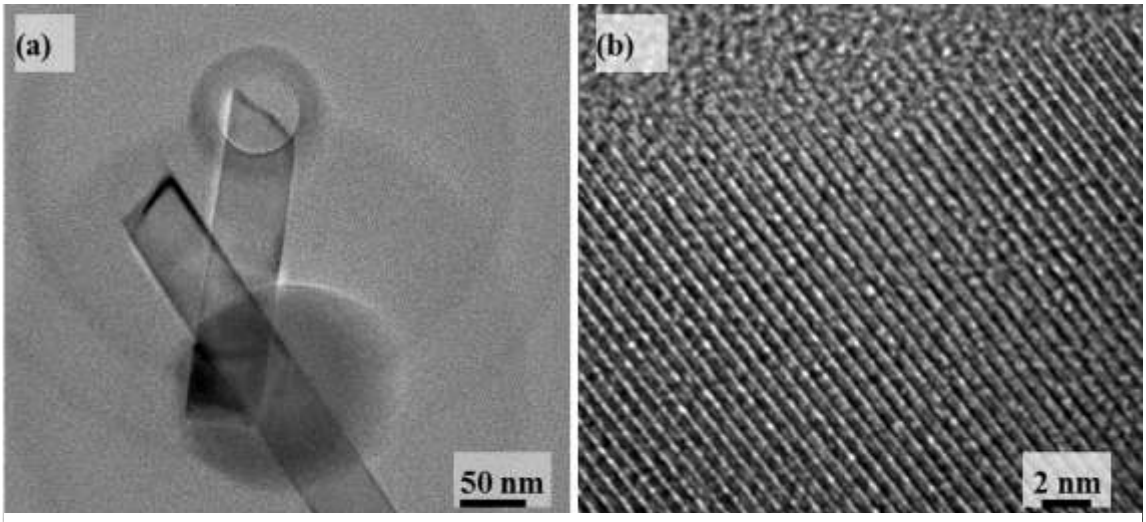

Figure 3.5. TEM images showing (a) low magnification, and (b) high resolution images of the GaN nanowires.

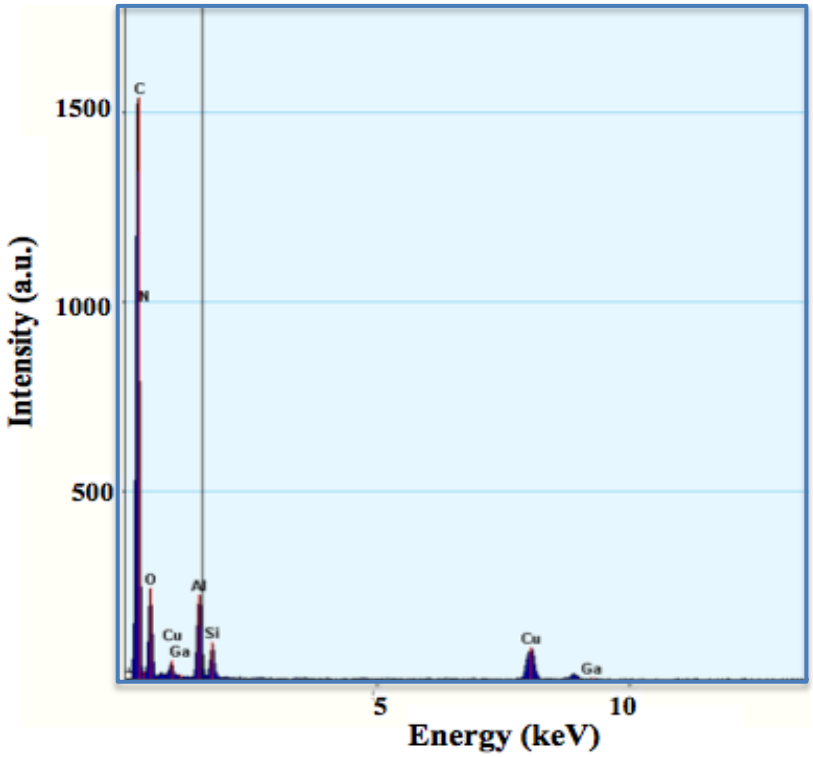

Figure 3.6. EDX composition of GaN nanowires.

3.1.2 GaN flower-like structures

After finding an optimized growth temperature for GaN nanowires, experiments were carried out to understand how the thickness of the catalyst influenced the growth of nanowires. The thickness of the Au catalyst layer was increased from 1 to 5 nm. The experiments were carried out at 850 ºC, with the same growth time, chamber pressure, and flow rates as previously mentioned. The temperature was set to 850 ºC because there is a temperature gradient from the center of the laser spot to the edge of the sample. By setting the temperature to 850 ºC, it was low enough not to obliterate the substrate, but hot enough that a large temperature spectrum was covered across the sample.

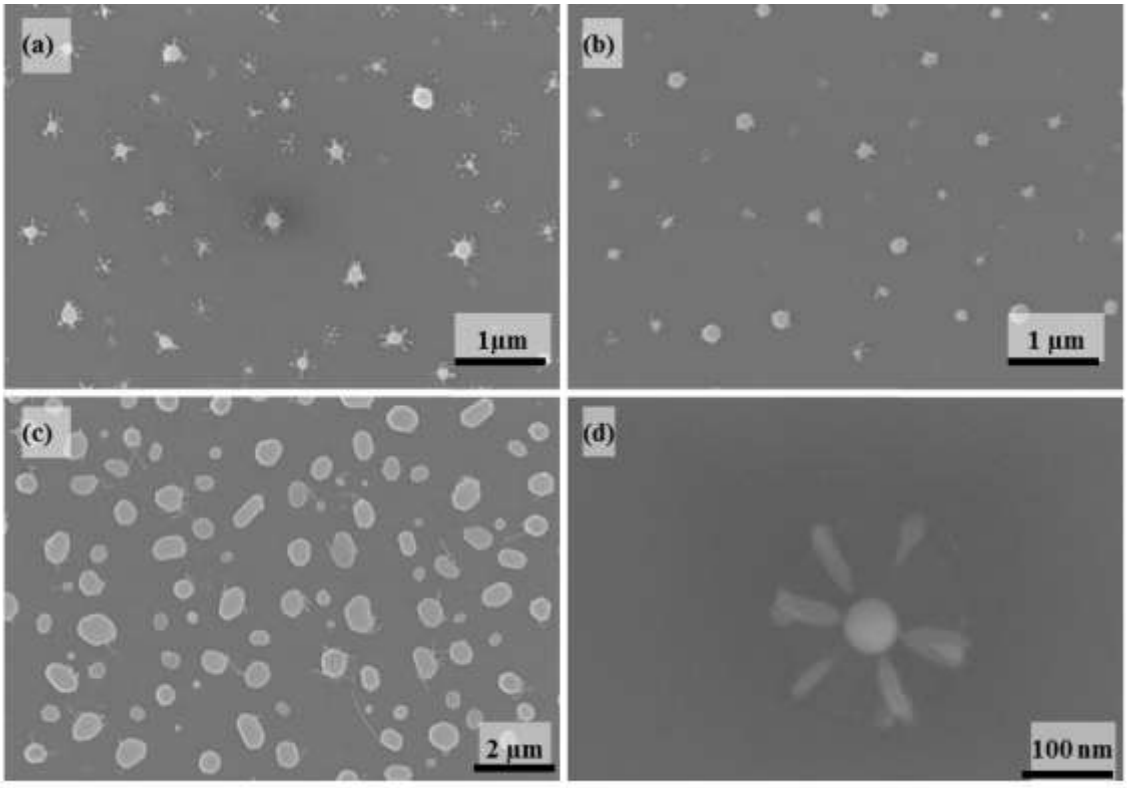

Figure 3.7. SEM images of flower-like structures in (a) center of laser spot where temperature is highest, (b) outside edge of laser spot, (c) edge of substrate where temperature is lowest. Figure (d) shows a magnified view of a nano-flower.

Figures 3.7 (a-c) show the structures formed as a result of the experiment in the center of the laser spot, at the edge of the laser spot, and at the edge of the sample, respectively. Figure 3.7 (d) shows a zoomed in view of one of the structures found in (a). Formation of the nano-flowers can be seen that in the center and right on the edge of the laser spot, where the temperature is highest. These structures consist of a ‘dot’-like structure ranging in diameter from 30 to 100 nm, with six ‘petals’ protruding from the edges. The six petals may be linked to the hexagonal structure of GaN, but more investigation is needed to support these claims. Outside of the laser spot, where the temperature was much lower, islands of diameter 1 – 2 μm can be found with a hand full of nanowires ranging in length from 1 to 2 μm. These results show that 5 nm of Au

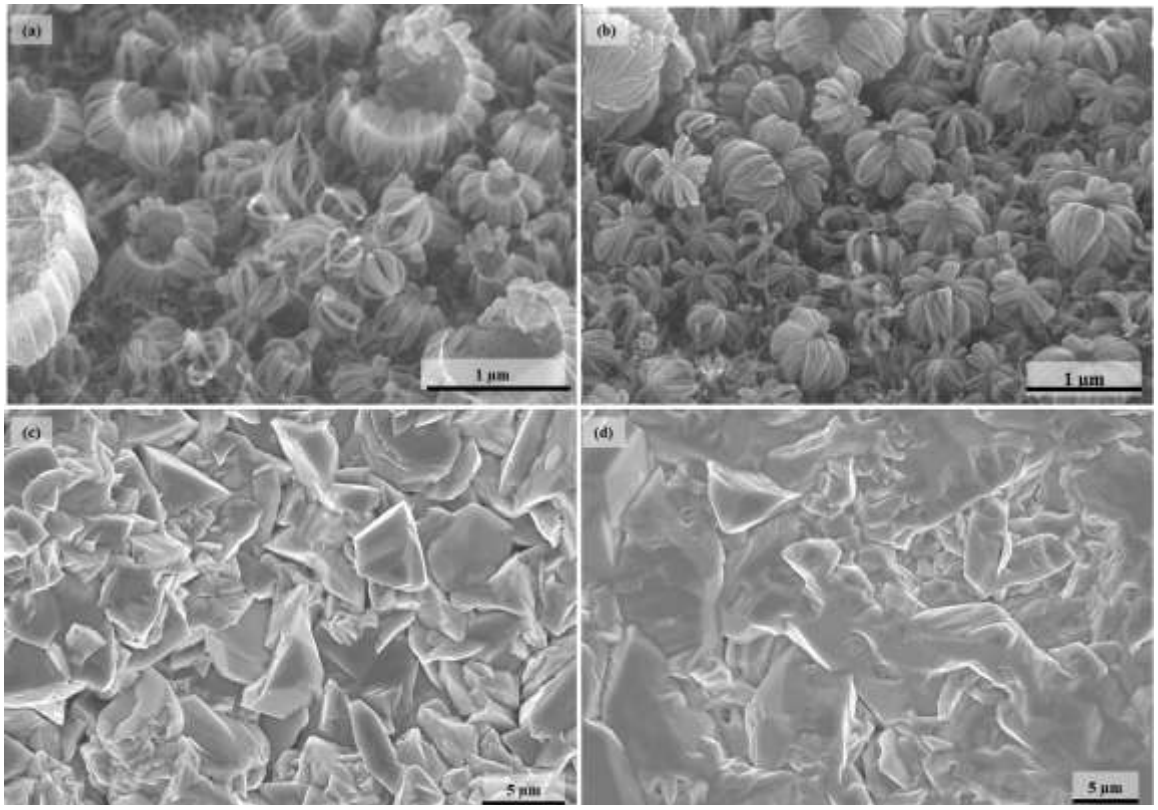

Figure 3.8. (a,b) GaN nano-flowers and (c,d) GaN crystals grown on the same Si substrate.

catalyst does no result in growth of nanowires, and thinner Au catalyst layers are needed for the abundant growth of GaN nanowires.

In addition to the small flower-like structures, larger, more defined floral structures were found. The experimental parameters for these results are as follows: 30 sccm of NH_3, 18 sccm of TMGa, chamber pressure of 600 Torr, substrate temperature maintained at 850 ºC, and the experiment time was 2 min. With these growth parameters, two very different morphologies were found on different areas of the substrate, the FE-SEM images for both can be found in Fig. 3.8. Outside of the laser spot, where the temperature was lower, large detailed floral structures were found ranging in diameter from ~200 to ~500 nm. These structures were found very close to the location where the tungsten sample holder comes in contact with the substrate, so the tungsten substrate holder might have an influence on the formation of the GaN flower-like structures. More

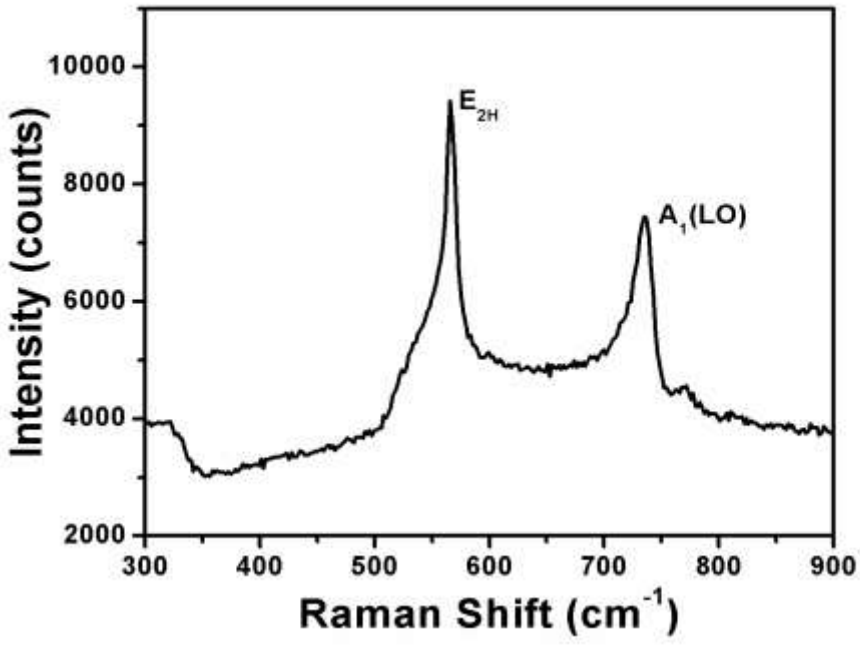

Figure 3.9. Raman spectrum obtained from crystal structure grown in the center of the laser spot.

experiments are needed in order to understand the evolution of these GaN nanostructures.

Further from the tungsten holder, inside the laser spot, large (~5-10 μm) crystals can be seen. These structures were grown at a higher temperature, and without the influence of the tungsten holder. Raman data was collected from the sample can be seen in Fig. 3.9. It shows a fairly large peak at 726 cm^{-1}, which corresponds with the A_1(LO) peak, and a very strong E_{2H} peak at 570 cm^{-1}. This indicates that the as-grown GaN crystals are of very high crystalline quality.

3.1.3 Nano-pillars

From previous experiments, it was found that the optimized growth of nanowires occurred at 750 ºC with 1 nm of Au catalyst. Additional experiments were carried out using these parameters, as well as a NH_3 flow rate of 30 sccm, chamber pressure of 600 Torr, experiment time of 10 min, and TMGa flow rate of 15 sccm. In these growth conditions, GaN pillar-like-structures were found, as shown in Fig 3.10. The FE-SEM images show that like nanowires, nano-pillars have a triangular cross section. Unlike nanowires, nano-pillars have a wide base of ~ 100 to 200 nm, and taper to a sharp point at the end.

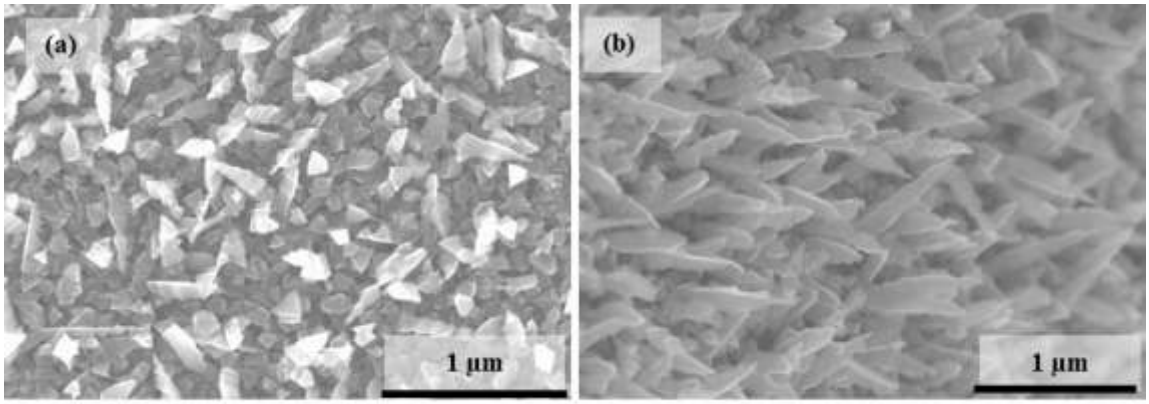

Figure 3.10. GaN nano-pillars (a) aerial view and (b) side view.

3.1.4 Patterned Growth

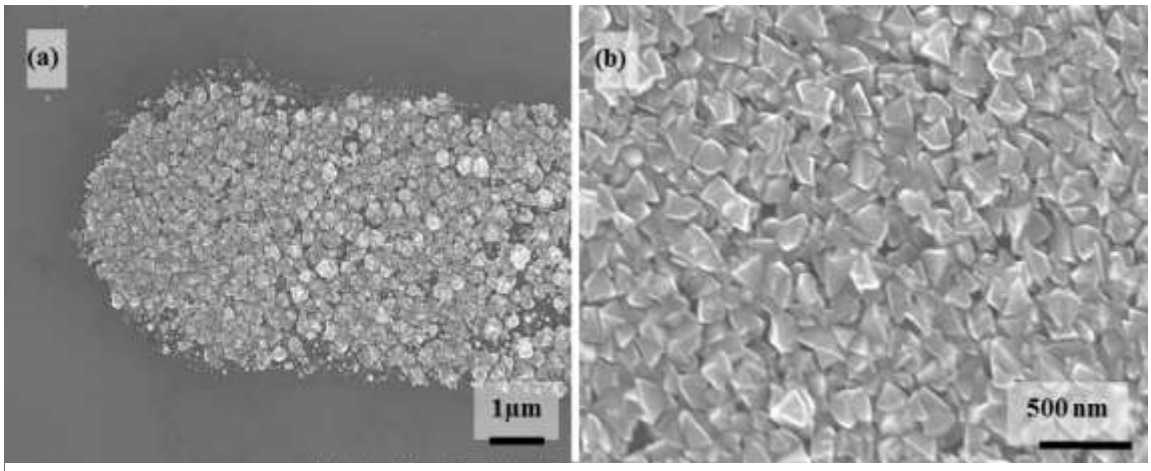

Figure 3.11. FE-SEM image of GaN grown only on patterned Si/SiO_2 substrate.

Included in the project goal of attaining nanowires is to achieve controlled, aligned growth of GaN in order to broaden potential applications. The first step in this process is to achieve GaN growth in specific, predetermined areas. In order to do this, patterned Si/SiO_2 samples (as described in Chapter 2) with a 5-nm-thick iron catalyst layer were used. The experiments were carried out with NH_3 flowing at 30 sccm, TMGa flowing at 10 sccm, growth temperature of 750 ºC, at a chamber pressure of 600 Torr. The FE-SEM results can be seen in Fig. 3.11. Although this is almost the same set of parameters used previously to achieve GaN nanowires, the Al-Fe-Al bimetallic catalyst layer led to the growth of grain-like nanocrystals. These crystals range in size from ~100 to ~300 nm. The growth of the crystals is limited to the area in which the catalyst layer was deposited. The patterned growth of GaN is important because it shows that under the right condition, the growth location of GaN can be controlled.

Additional experiments were carried out on the patterned substrates with the following parameters: NH_3 flow rate of 30 sccm, TMGa flow rate of 0.5 sccm, chamber

pressure of 500 Torr, and substrate temperature of 700 ºC. The results of these experiments can be seen in Fig. 3.12. Figure 3.12 (a) shows the FE-SEM images which contain hexagonal crystal structures ranging in diameter from 200 to 500 nm, as well as bundled nano-pillars with thicknesses around 50 nm and lengths around 500 nm. Raman data was also collected on these structures, and is found in Figure 3.12 (b). The Raman results show strong peaks of the E_{2H} and A_1(LO) modes, meaning the crystallinity of the hexagonal crystals and nano-pillars is good.

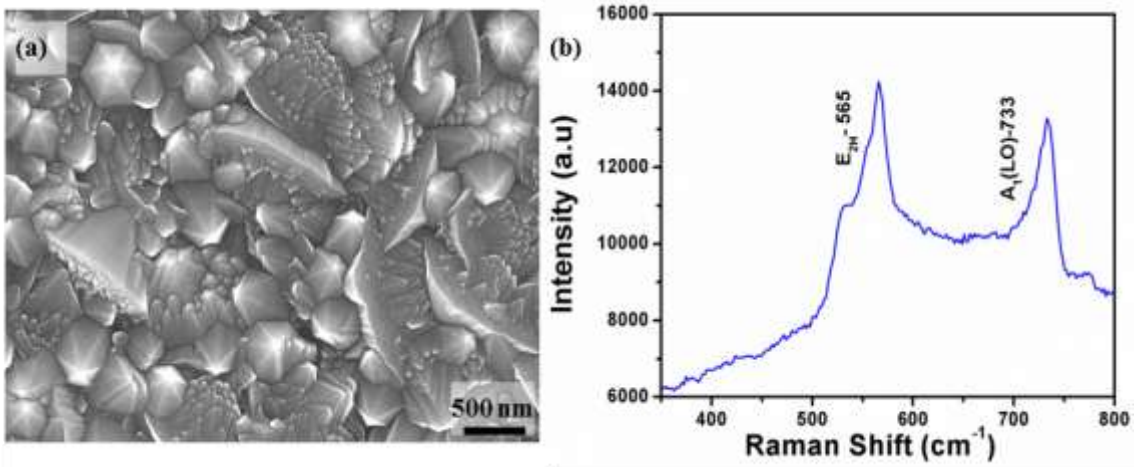

Figure 3.12. (a) FE-SEM image and (b) Raman spectrum of hexagonal GaN crystals.

3.2 GaN Polycrystalline Thin Films

The second major task of this project is to synthesize epitaxial layers of GaN. For this portion of the project, experiments were carried out on bare Si and Si/SiO_2 substrates without any substrate coating. The polycrystalline GaN thin films were deposited on a bare Si substrate (prepared as described in Chapter 2) using the following parameters: NH_3 flow rate of 30 sccm, substrate temperature of 850 ºC, chamber pressure of 600 torr, experiment time of 10 min, and the TMGa flow rate was varied at 12, 15, and 18 sccm.

Figure 3.13 shows the resulting FE-SEM micrographs. It can be seen that large, overlapping crystal structures were formed in these experiments. The crystal size ranges from ~5 to ~ 20 µm, with the smallest of the crystals being found at a TMGa flow rate of 12 sccm.

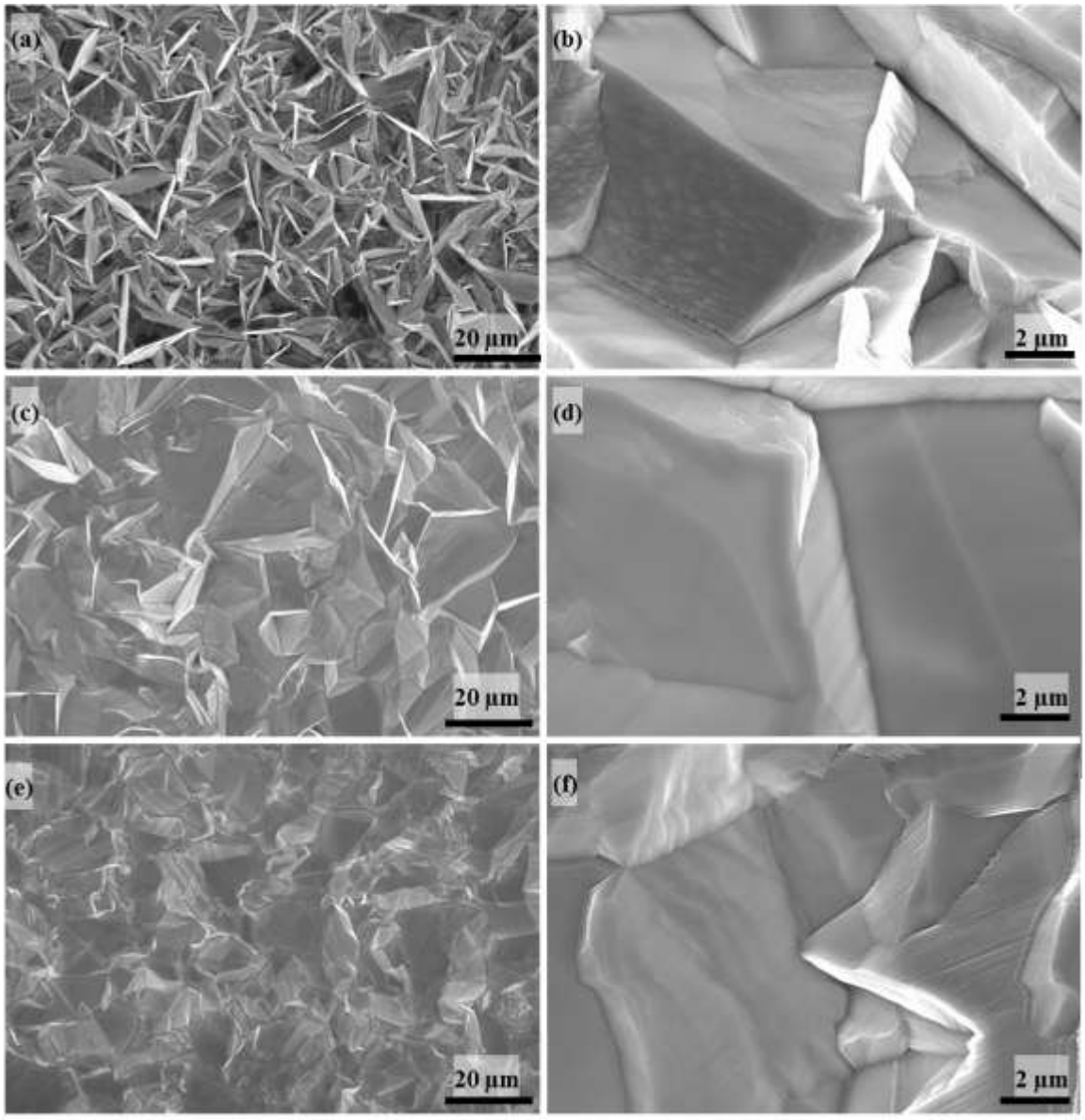

Figure 3.13. FE-SEM image of GaN thin films grown at varying TMGa flow (a) 12 sccm (c) 15 sccm and (e) 18 sccm. (b, d, f) 2 µm scale view of figure a, c, e, respectively.

In addition to FE-SEM, Raman data was also collected for these samples, and can be found in Fig. 3.14. Peaks can be seen in the Raman spectra at 534, 568, 739 and 768 cm^{-1}, which correspond to the E_{2H}, $A_1(LO)$, $E_1(LO)$ and $A_1(TO)$ modes of GaN, respectively. The prominent E_{2H} mode is characteristic of the wurtzite crystal structure, and confirms that the layers grown are, in fact, GaN. The strongest E_{2H} peak can be found in the spectra corresponding to the film achieved with a TMGa flow rate of 18 sccm meaning that the higher TMGa flow rate produces higher quality crystals.

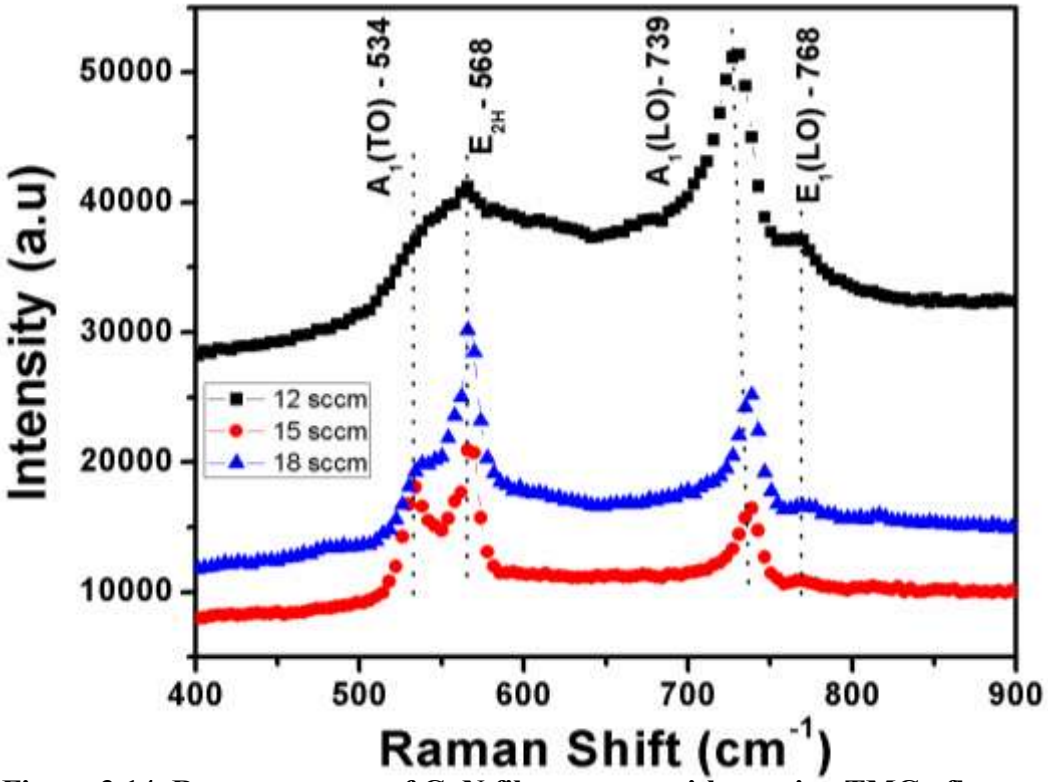

Figure 3.14. Raman spectra of GaN films grown with varying TMGa flow rates.

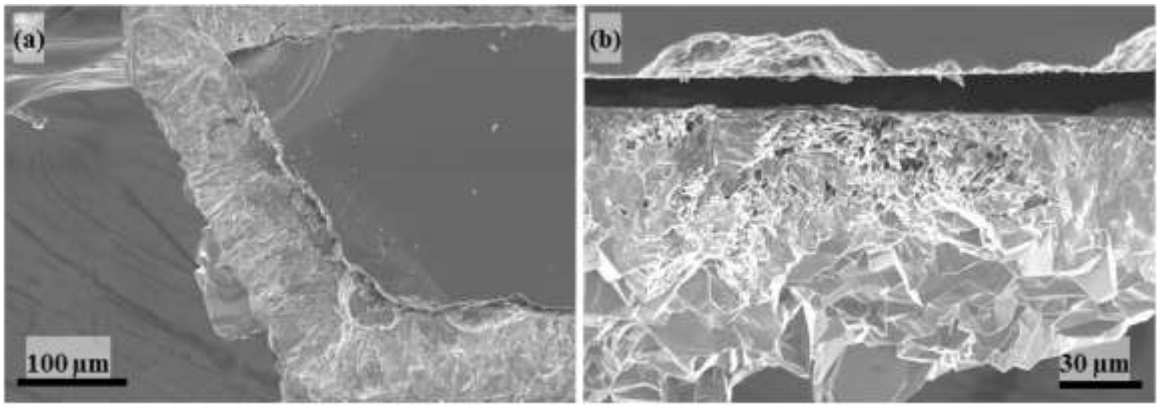

Figure 3.15. Cross-sectional FE-SEM image of GaN thin films grown at 15 sccm.

To investigate the thickness of the layers, cross-sectional FE-SEM was carried out. The sample was split down the middle using a diamond-tipped cutting tool, and the sample was aligned vertically in the FE-SEM sample holder. Figure 3.15 shows the

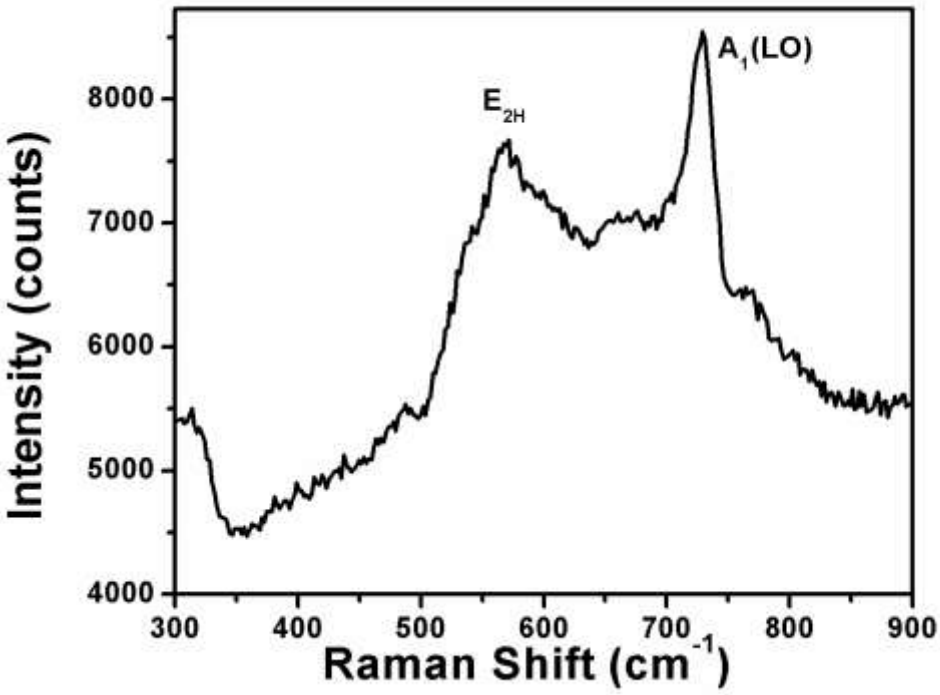

Figure 3.16. Cross sectional Raman from GaN synthesized with 15 sccm TMGa.

micrographs obtained in the cross-sectional analysis. It can be seen that the film thickness varied between 80 and 100 µm. This thickness was obtained during a 10-min experiment, meaning the growth rate for the sample is roughly 500 to 600 µm/hour. This result is much higher than previously reported values for MOVPE, LPE, and MBE, and it rivals reported values for HVPE as discussed in Chapter 1. With the sample split, cross sectional Raman was also carried out. The results from the Raman, shown in Figure 3.16 show peaks in the same location with the same relative strengths as the top down Raman. This indicates that the crystalline quality is high throughout the thickness of the crystal.

The compositions of the GaN polycrystalline thin films were examined using LIBS. The resulting spectrum showed very strong peaks at 403.2, 417.6, and 428.9 nm which are characteristic gallium peaks. Also found on the sample was a relatively small peak at 409.9 nm, which is associated with nitrogen. Although this peak is small, it is still significant, and shows the composition of the film grown contains only gallium and nitrogen. Spectral acquisitions from the LIBS experiments can be found in Fig. 3.17.

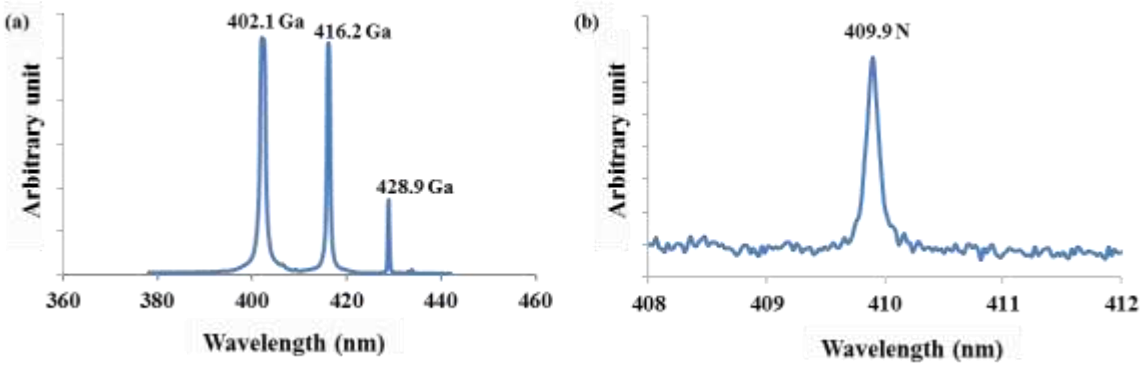

Figure 3.17. LIBS spectra showing (a) gallium peaks and (b) nitrogen peaks

Finally, in order to see why large, overlapping crystals were formed as opposed to epitaxial layers, short-duration experiments were carried out. The parameters were set to NH_3 flow rate of 30 sccm, substrate temperature of 850 ºC, chamber pressure of 600 Torr, TMGa flow rate of 18 sccm (the optimized condition from above), but the time was

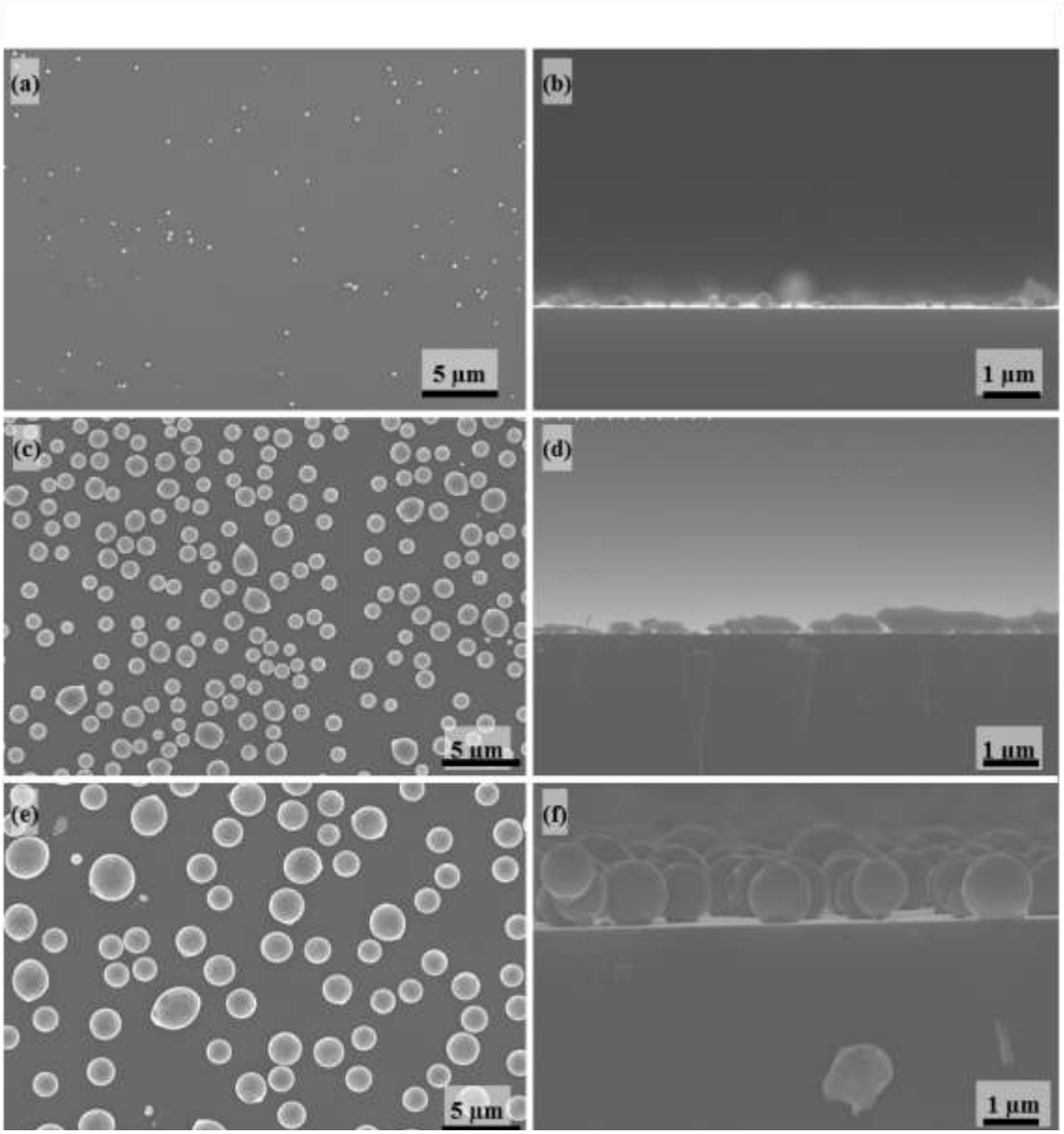

Figure 3.18. FE-SEM image of GaN thin films grown at a varying time. (a) 30 seconds, (c) 60 seconds, (e) 90 seconds. (b, d, f) cross-sectional view of a, c, e, respectively.

lowered from 10 min to 30, 60, and 90 sec. The short experiment time allowed for further study of the nucleation stage of GaN crystals.

Figure 3.18 shows both top-down and cross-sectional FE-SEM images gathered from these samples. The micrographs show that in the first 30 sec of the experiment, small islands with diameter ~ 200 nm begin forming on the surface of the substrate. As time increases, there is an increase in both the abundance and size of the islands. For the GaN films grown at 90 sec, the islands range in diameter from 2 to 4 μm. Figure 3.19 shows zoomed in view of one of the large islands grown for 90 sec. It is noted that a hexagonally facetted structure can be seen growing from the island. It is believed that as the experimental time increases, these facet structures grow from the islands and begin overlapping, as seen in Fig. 3.19 (a). As the growth time increases further, the islands grow into the crystals found in Figure 3.13.

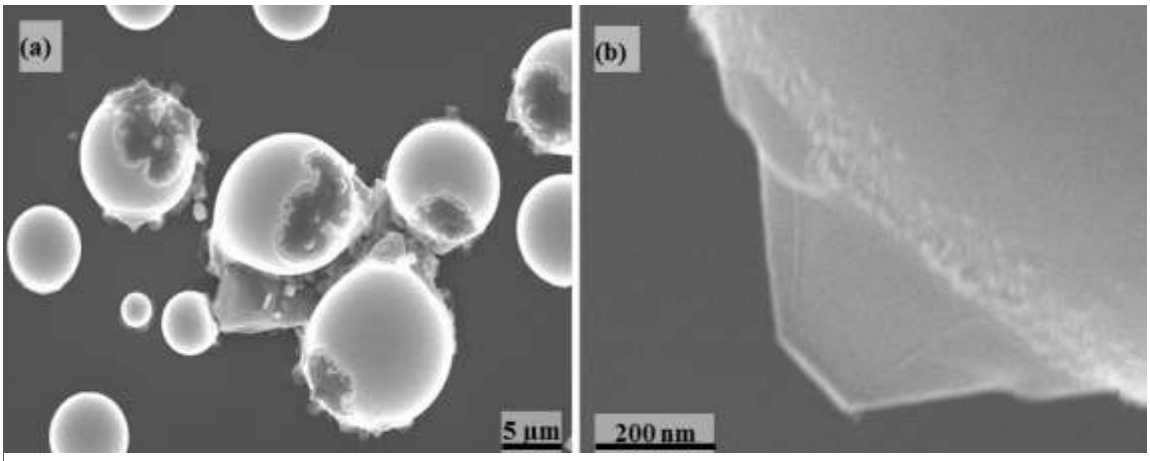

Figure 3.19. FE-SEM image of (a) nano island combining, and (b) magnified image of GaN grown for 90 sec.

Chapter 4

Conclusion and Recommendations for Future Work

4.1 Conclusions

In this research, an L-MOVPE system was designed and built in order to take advantage of the localized heating associated with a CO_2 laser, and synthesize GaN at low substrate temperatures. Experiments were carried out to study the growth of GaN nanostructures and thin films, and how parameters like precursor flow rates, substrate temperature, chamber pressure, and experiment duration affect the structure and quality of GaN grown. The morphology of the structures was then characterized using FE-SEM and TEM. The crystallinity and composition were examined through Raman spectroscopy and LIBS. Through this characterization, it was found that the L-MOVPE

method is capable of achieving numerous morphologies of GaN including nanowires, nano-pillars, nano-flowers, grain-like crystals, and polycrystalline thin films.

The results show GaN nanowires were grown with lengths ~2 μm and widths ~20 nm. These nanowires have large A_1(LO) peaks and small E_{2H} peaks indicating that the crystalline quality of the GaN is not excellent. In addition to nanowires, morphologies like GaN nano-pillars and flower-like structures were realized at different growth parameters. Several sizes of GaN crystals (microcrystal and nanocrystals) were grown using the L-MOVPE ranging from grain-like (~40 nm) to large overlapping crystals (~40 μm). All crystal structures grown exhibit strong GaN peaks in the Raman spectrum, with the highest E_{2H} peak occurring when the TMGa flow rate was at a system maximum 18 sccm. This indicates the crystallinity of the GaN increases as the TMGa flow increases. The large overlapping crystals were shown to have a growth rate of ~500 – 600 μm/ hour, which is much higher than the reported growth rates associated with traditional MOVPE, LBE, and MBE. It was also found that these large crystal structures form from small islands. The islands were shown to increase in diameter from ~500 nm to ~2.5 μm as experiment time increases from 30 to 90 sec. In time, the islands sprout facetted crystal-like structures, which eventually grow in size, and become the overlapping crystals mentioned previously.

Overall, this research showed the versatility of the L-MOVPE method, which is able to synthesize different morphologies of GaN at low substrate temperatures. Experiments were carried out to find optimized parameters for achieving specific GaN nano-structures, and the groundwork was laid for continued research and advancement in the growth of GaN using a novel L-MOVPE approach.

4.2 Recommendation for Future Work

Because the overall scope of this project is so large, there is quite a bit left to do. To begin, the CO_2 laser for the system should be replaced with a wavelength tunable laser. Rather than rely solely on heat for the decomposition of NH_3, a tunable CO_2 laser can be set to a wavelength which will resonantly excite the ν_2 umbrella mode of the NH_3 molecules[36]. Figure 4.1(a) shows the schematic representation of the CO_2 laser exciting the vibrational modes of NH_3, and Figure 4.1(b) shows the absorption coefficients of NH_3 at the CO_2 laser $00^o1\text{-}10^o0$ emission band which corresponds with 10.4 μm [36]. It can be seen that the peak absorption occurs at 10.333 and 10.719 μm. By using the CO_2 laser to

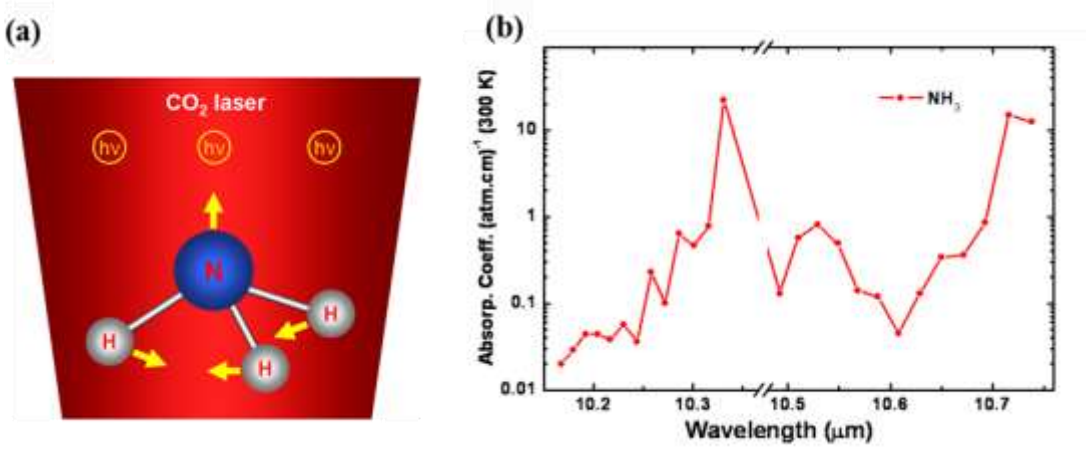

Figure 4.1. (a) Schematic diagram of CO_2 laser excitation of NH_3 vibrational modes. (b) Absorption coefficients of NH_3 gas at the CO_2 laser $00^o1\text{-}10^o0$ emission band.

efficiently dislocate the N-H bonds, less energy and lower temperatures are needed to carry out the synthesis of GaN. This novel approach can also be extended to the growth of III-Nitride materials such as AlN, InN, AlGaN and InGaN. In this project, continued study is needed into the nucleation stage for the growth of epitaxial layers. Learning how the crystals form will allow for greater control over the growth of the epitaxial layer.

Once GaN epitaxial layers are achieved, this method can be extended to other III-Nitride materials such as aluminum nitride and indium nitride by simply changing the precursor gas from TMGa to TMAl or TMIn.

For the nanowire experiments, the next step would be to achieve aligned growth of nanowires. As stated, the MOVPE system was fitted with a BNC connector, which will allow an electric field to be applied to the electrodes of patterned substrates through the tungsten sample holder. A large electric field generated by a DC power supply should help to facilitate aligned growth. This process has already been demonstrated through the realization of aligned growth of carbon nanotubes in previous research in the Laser-Assisted Nano Engineering Lab [30]. Once aligned growth is achieved, the remaining step is to dope the GaN nanowires. Because the MOVPE setup was built in-house, it is completely customizable, which will allow the addition of a dopant such as Mg (p-type GaN), Al and Si (n-type GaN) . With proper doping levels, the GaN nanowires will be able to achieve emission of light all across the visible spectrum.

References

[1] H. M. Kim, High-brightness light emitting diodes using dislocation-free indium gallium nitride/gallium nitride multiquantum-well nanorod arrays. *Nano Lett* **4**, 1059-1062 (2004).

[2] A. Perez-Tomas, GaN transistor characteristics at elevated temperatures. *Journal of Applied Physics*, **106**(7), 074519- 074519-7, (2009).

[3] M. E. Levinshteĭn, Properties of advanced semiconductor materials : GaN, AlN, InN, BN, SiC, SiGe. *Wiley* (2001).

[4] S. Adachi, Physical properties of III-V semiconductor compounds : InP, InAs, GaAs, GaP, InGaAs, and InGaAsP. *Wiley* (1992).

[5] H. Xu, Fabrication and Electrical/ Optical Characterixation of Bulk GaN-based Schottky Diodes, *Doctoral Dissertation,* 2-14 (2009).

[6] B. Gil, Valence-band physics and the optical properties of GaN epilayers grown onto sapphire with wurtzite symmetry. Phys. Rev. B **52,** R17028–R17031 (1995).

[7] D.A. Steigerwald, Illumination with solid-state lighting technology. *Selected Topics in Quantum Electronics*, **8**(2), 310-320, (2002).

[8] M. Koike, Development of high efficiency GaN-based multiquantum-well light-emitting diodes and their applications, *IEE Journal of Selected topics in Quantum Electronics*, **8**(2), 271-277, (2002).

[9] W.P. Risk, Diode laser pumped blue-light source at 473 nm using intracavity frequency doubling of a 946 nm Nd: YAG laser. *App. Phy. Letters,* **54**(17), 1625-162, (1989).

[10] S. Nakamura, InGaN/GaN/AlGaN-based laser diodes with modulation-doped strained-layer superlattices grown on an epitaxially laterally overgrown GaN substrate. *Appl. Phys. Lett.* **72**, 211 (1998).

[11] O. H. Nam, Characteristics of GaN-based laser diodes for post-DVD applications. *Physica status solidi* **201**(12), 2712-2720, (2004).

[12] LED 5MM. Digi-Key Corporation. 2012. <http://parts.digikey.com/1/parts/1571115-led-5mm-green-clear-527nm-15deg-c503b-gan-cb0f0791.html>

[13] Diode Laser Modules. Riothner Laser. 2012 <http://www.roithner-laser.com/lasermodules/laser_modules405.html>

[14] Trans 120W RF GaN HEMT. Digi-Key Corporation. 2012. <http://parts.digikey.com/1/parts/1661527-trans-120w-rf-gan-hemt-440193pkg-cgh40120f.html>

[15] W. Saito, High breakdown voltage AlGaN-GaN power-HEMT design and high current density switching behavior. *IEEE transactions on electron devices*, **50** 2528-2531 (2003).

[16] S. Y. Lee, Water-resistant flexible GaN LED on a liquid crystal polymer substrate for implantable biomedical applications. *Nano Energy,* (2011).

[17] Y. Dora, High Breakdown Voltage Achieved on AlGaN/GaN HEMTs With Integrated Slant Field Plates. *IEEE Electron Device Letters* **27** (9): 713 (2006).

[18] H. Morkoc, Large-band-gap SiC, III-V nitride, and II-VI ZnSe-based semiconductor device technologies. *Journal of Applied Physics* **76** (3): 1363 (1996).

[19] Z. Yang, GaN grown by molecular beam epitaxy at high growth rates using ammonia as the nitrogen source. *App Phy Lett* **67**(12) , 1686-1688, (1995).

[20] T. Paskova, Growth, Separation and Properties of HVPE Grown GaN Films using Different Nucleation Schemes. *IPAP Conf. Series* **4**, 14-22, (2002).

[21] F. Kawamura, Growth of large GaN single crystal using the liquid phase epitaxy (LPE) technique. *Japanese Journal of Applied Physics*, **42**, L4-L6 (2003).

[22] S. A. Safvi, GaN Growth by Metallorganic Vapor Phase Epitaxy. *Journal of the Electrochemical Society* **144**, 1789-1796, (1997).

[23] Namokhyeon, MOCVD Basics and Applications. *Samsung Advanced Institute of Technology*. 1-63, (2004).

[24] L. H. Long, The heat of formation and physical properties of gallium trimethyl. *Trans. Faraday Soc.* **54**, 1797-1803 (1958).

[25] A. Hirako, Decomposition and Uniformity of Material Gases in GaN MOVPE. *physica status solidi*, 489-493 (2002).

[26] A. Kuramata, High quality GaN epitaxial layer grown by metalorganic vapor phase epitaxy on (111) $MgAl_2O_4$ substrate. *Appl. Phys. Lett.* **67**, 2521 (1995).

[27] A. F. Wright, Consistent structural properties for AlN, GaN, and InN. *Phys. Rev. B.* **51**(12), (1995).

[28] K. Hiramatsu, Relaxation Mechanism of Thermal Stresses in the Heterostructure of GaN Grown on Sapphire by Vapor Phase Epitaxy. *Jpn. J. Appl. Phy* **32**, 1528-1533, (1993).

[29] F. Sedky, Experimental determination of the Maximum post-process Annealing Temperature for standard CMOS wafers. *IEEE Transactions on Electron Devices,* **48** (2), 377-384, (2001).

[30] Y. Gao, Controlled growth of carbon nanotubes on electrodes under different bias polarity. *Appl Phys Lett* **95**, (2009).

[31] J. R. Ferraro, Introductory Raman Spectroscopy, *Academic Press,* 2-91, (2002).

[32] P. Flewitt, Physical Methods for Materials Characterization: Second Addition. *IOP Series in Materials Science and Engineering,* 274-394 (2003).

[33] A. Miziolek, Laser-induced breakdown Spectroscopy: Fundamentals and Applications. *Cambridge University Press,* (2006).

[34] S. Zhang, Materials Characterization Techniques, *CRC Press.* 153-205, (2009).

[35] R. Agarwal, Semiconductor nanowires: optics and optoelectronics. Appl Phys a-Matter **85**, 209-215 (2006).

[36] F. Gatti, Fully coupled 6D calculations of the ammonia vibration-inversion-tunneling states with a split Hamiltonian pseudospectral approach. *J Chem Phys **111***, 7236-7243 (1999).

[37] R. R. Patty, Carbon dioxide laser absorption coefficients for determining ambient levels of O3, NH3, and C2H4. *Appl Opt* **13**, 2850-2854 (1974).

[38] H. Harima, Properties of GaN and related compounds studied by means of Raman scattering. *Journal of Physics: Condensed Matter* **14**, R967- R993 (2002).

[39] B. Łucznik, Deposition of thick GaN layers by HVPE on the pressure grown GaN substrates. *Journal of Crystal Growth,* **281,** 38-46 (2005).

[40] F. Kawamura, Growth of large GaN single crystal using the liquid phase epitaxy (LPE) technique. *Japanese Journal of Applied Physics*, **42**, L4-L6 (2003).

[41] R. Q. Hui, III-nitride-based planar lightwave circuits for long wavelength optical communications. *IEEE J Quantum Elect* **41**, 100-110 (2005).

[42] J. W. Lee, Dielectrophoretic assembly of GaN nanowires for UV sensor applications. *Solid State Commun* **148**, 194-198, (2008).

[43] K. W. Chang, Low-temperature catalytic synthesis gallium nitride nanowires. *J Phys Chem B* **106**, 7796-7799 (2002).

[44] H. Ling, Enhanced chemical vapor deposition of diamond by wavelength-matched vibrational excitations of ethylene molecules using tunable CO2 laser irradiation. *J Appl Phys* **105**, - (2009).

[45] N. R. Franklin, An enhanced CVD approach to extensive nanotube networks with directionality. *Adv Mater* **12**, 890-894 (2000).

[46] L. H. Liu, Infrared and Raman-scattering studies in single-crystalline GaN nanowires. *Chem Phys Lett* **345**, 245-251 (2001).

[47] V. M. Apatin, Study of nitrogen isotope-selective two-stage IR plus UV dissociation of ammonia molecules. *High Energ Chem+* **42**, 409-417, (2008).